

Late Cenozoic erosion estimates for the northern Barents Sea: Quantifying glacial sediment input to the Arctic Ocean

Amando Lasabuda^{1,2}, Wolfram H. Geissler³, Jan Sverre Laberg^{2,1}, Stig-Morten Knutsen^{4,1}, Tom Arne Rydningen², and Kai Berglar⁵

¹Research Centre for Arctic Petroleum Exploration (ARCEX), Department of Geosciences, UiT – The Arctic University of Norway, 9037 Tromsø, Norway

²Department of Geosciences, UiT – The Arctic University of Norway, 9037 Tromsø, Norway

³Alfred-Wegener-Institut Helmholtz-Zentrum für Polar- und Meeresforschung (AWI), Am Alten Hafen 26, D-27568 Bremerhaven, Germany

⁴Norwegian Petroleum Directorate (NPD), Storgata 49, 9406 Harstad, Norway

⁵Federal Institute for Geosciences and Natural Resources (BGR), Hannover, Germany

Corresponding author: Amando Lasabuda (amando.lasabuda@uit.no)

Key Points:

- Quantification of the glacial sediment input to the Arctic Ocean from the northwestern Barents Sea
- For the first time, average erosion and erosion rates are estimated from the source area of this margin using the mass balance approach.
- These rates are comparable to those reported from other glaciated margin, but only about half compared to the western Barents Sea margin.

This article has been accepted for publication and undergone full peer review but has not been through the copyediting, typesetting, pagination and proofreading process which may lead to differences between this version and the Version of Record. Please cite this article as doi: 10.1029/2018GC007882

Abstract

A compilation of seismic data has been used to characterize the Neogene – Quaternary sedimentary succession of the northwestern Barents Sea continental margin to better understand the paleoenvironmental evolution and the sedimentary processes involved. The Neogene strata are dominated by contourites related to the ocean circulation established from the opening of the Fram Strait connecting the Atlantic and the Arctic Oceans (< ~17.5 Ma). The upper Plio–Pleistocene strata (< ~2.7 Ma) are dominated by stacked gravity-driven deposits forming trough-mouth fans that were sourced from paleo-ice streams. Within the inter-fan areas, contouritic sedimentation prevailed. Thus, this margin provides an example of interaction of glacial debris flows, contour currents, and hemipelagic/glacimarine sedimentary processes. A total of ~29,000 km³ of sediments with an average sedimentation rate of about 0.24 m/Kyr were estimated. These numbers reflect the sediment input to this part of the Arctic Ocean from the northwestern Barents Sea shelf and adjacent land areas. For the first time, the average erosion and erosion rates for this source area are estimated using a mass balance approach. Approximately 410 – 650 m of erosion has on average occurred, corresponding to an average erosion rate of ~0.15 – 0.24 m/Kyr. These rates are comparable to those reported from other glaciated margins, including the western Svalbard and mid-Norway margin, but up to only half the rates reported from the western Barents Sea margin. This variation is interpreted due to the size and bedrock types of the drainage area, ice dynamics, and the continental slope gradient.

Keywords: northwestern Barents Sea, late Cenozoic, glacial erosion, erosion rates

Accepted

1. Introduction

The Arctic Ocean and its constituent seas following the definition of the International Hydrographic Organization (2002) are in several aspects different from the other major oceans of the world. It is the shallowest ocean and has significantly larger continental shelves including the shelves of the Barents, Kara, and Laptev Seas. In total, the continental shelf area, from the coasts out to the shelf break, make up as much as ~52.9% of the total area in the Arctic Ocean (Jakobsson, 2002).

The Barents Sea mean depth is ca. 200 m and its largest seafloor area is located between 150 and 300 m. Shallow banks and overdeepened troughs ending at the shelf break dominate its seafloor morphology. A few large trough-mouth fans (TMFs) are located off the northern Barents Sea shelf including the Franz Victoria TMF (Figure 1). The present morphology and depth are mainly related to glacial erosion from ice streams within a grounded ice sheet repeatedly covering the continental shelf (e.g. Laberg et al., 2010). So far, no attempts have been made to quantify this erosion affecting the northern Barents Sea shelf and adjacent land areas.

Fast-flowing paleo-ice streams that occupied continental shelf troughs are identified as effective agents in eroding and transporting sediments to the shelf break, which have been documented from many formerly glaciated continental margins (e.g. Kuvaas & Kristoffersen, 1991; Faleide et al., 1996; King et al., 1996; Laberg & Vorren, 1996; Andreassen et al., 2008; Laberg et al., 2009; Vorren et al., 2011; Batchelor et al., 2013; Jakobsson et al., 2014; Dowdeswell et al., 2016; Rydningen et al., 2016). A slower-moving or sluggish ice is commonly present on the adjacent shallower banks delivering less sediments to the continental slope (Dowdeswell & Cofaigh, 2002; Ottesen et al., 2005; Dowdeswell et al., 2008; Rydningen et al., 2013). These slope areas, instead, may be dominated by contourites or contourite drifts (Eiken & Hinz, 1993; Laberg et al., 1999, 2001, 2005; Rebesco et al., 2014).

The glacial sediment accumulation in front of the troughs record massive, episodic sedimentation from ice streams through debris flows and their associated mass-wasting processes (e.g. Laberg & Vorren, 1995; Faleide et al., 1996; King et al., 1998; Vorren et al., 1998; Batchelor & Dowdeswell, 2014). The glacial debris flows are considered as the most important processes in TMF development. Sediments are transported by ice streams to the shelf break during full-glacial conditions, where they are deposited as a till-delta/diamict apron on the upper slope (e.g. Laberg & Vorren, 1995; King et al., 1996). These sediments are prone to instability and may collapse and travel downslope as debris flows. The deposits within TMFs have been regarded as palaeoclimatic archives that can be used to reconstruct the paleoenvironmental evolution and the Quaternary glacial history (e.g. Vorren & Laberg, 1997; Dahlgren et al., 2005; Laberg et al., 2010). In addition, they reflect the amount of glacial erosion in the drainage area (e.g. Laberg et al., 2012; Rydningen et al., 2016).

Contourite drifts deposited from along-slope ocean currents hold the potential to record the history of ocean circulation (Jakobsson et al., 2007). Also, their sedimentary succession is often prone to submarine failure (e.g. Vanneste et al., 2006; Winkelmann et al., 2008), and contourites seem to play a role in affecting the stability of the slope due to their composition, preferential location, and typical high water content (Canals et al., 2004; Laberg & Camerlenghi, 2008). Together, glacial-related mass-wasting processes and contour currents have contributed to the spatial variation and temporal evolution of formerly glaciated continental margins, forming their present-day morphology (e.g. Mosher et al., 2017; Pérez & Nielsen, 2017).

Medium to good quality seismic data of regional coverage have allowed us to better study the northwestern Barents Sea continental margin, including its glacial strata and sedimentary style that so far had not been studied in detail beyond the Last Glacial Maximum

(LGM). We use recently acquired multi-channel seismic data from various sources (Geissler & Jokat, 2004; Engen et al., 2009; Geissler et al., 2014; Berglar et al., 2016) to investigate the distribution of the Neogene – Quaternary deposits within the continental shelf, slope, and the adjacent deep-sea basin. The sedimentary processes are discussed based on seismic facies analysis focusing on the TMF development and a buried mega slide. For the first time in this area, average net glacial erosion and glacial erosion rates are estimated using the mass balance approach. The results are compared to similar studies from other glaciated margins to better understand the late Cenozoic uplift and erosion of the greater Barents Sea area (Nyland et al., 1992; Riis & Fjeldskaar, 1992; Lasabuda, 2018).

2. Geological setting

2.1. Structural elements and geodynamic evolution

The Arctic Ocean consists of two major depocenters, the Amerasia and Eurasia basins, separated by the Lomonosov Ridge (Figure 1). The basin configuration of the Arctic Ocean has evolved since the Mesozoic (Karasik, 1968; Vogt & Avery, 1974; Srivastava, 1985). The Eurasia Basin, comprising the Amundsen and Nansen basins is associated with continental breakup and subsequent seafloor spreading approximately at the Paleocene–Eocene transition (~55 Ma) (Talwani & Eldholm, 1977; Srivastava & Tapscott, 1986), although an earlier start of spreading, around magnetic anomaly 25 (~57 Ma) is proposed by Brozena et al. (2003). This event involved separation of the Lomonosov Ridge from the northern Barents Sea shelf, which was initiated by right-lateral movement (Minakov et al., 2013; Berglar et al., 2016). The Gakkel Ridge, which separates the Amundsen and Nansen basins, is characterized as an ultraslow spreading ridge (0.63-1.3 cm/yr) (Jokat & Micksch, 2004). The Yermak Plateau is located in the western part of the Arctic Ocean off northern Svalbard and is likely a stretched piece of continental crust of non-volcanic origin (Geissler et al., 2011). The conjugate Morris Jesup Rise on the northern Greenland margin was separated from the Yermak Plateau in the Oligocene (Jackson et al., 1984; Jokat et al., 2008). Initially, the Yermak Plateau and the Morris Jesup Rise formed a continuous feature prior to the plate reorganization at anomaly 13 time from which Greenland moved in the same direction as the North American plate (Talwani & Eldholm, 1977; Jackson et al., 1984).

The opening of the Fram Strait during the Miocene allowed deep-water exchange between the Atlantic and the Arctic oceans (Kristoffersen, 1990; Jakobsson et al., 2007; Engen et al., 2008; Jokat et al., 2016; Hein et al., 2017). The present-day West Spitsbergen Current continues eastwards into the Arctic Ocean (Manley et al., 1992). Contourite drifts deposited from these ocean currents are well-developed along the western Svalbard margin, the western slope of the Yermak Plateau (Geissler et al., 2011; Gebhardt et al., 2014), and further north in the central Arctic Ocean (Jokat, 2005; Jakobsson et al., 2007).

2.2. Glaciations and Barents Sea uplift and erosion

The greater Barents Sea area experienced extensive glaciations in the Plio–Pleistocene resulting in sediment transport towards the surrounding oceanic basins including the Nansen Basin (e.g. Elverhøi et al., 1998; Vorren et al., 2011). The term late Cenozoic in this study refers to the glacial period of this area from ~2.7 Ma to the Present, although recent results indicate the initial presence of local ice over Svalbard already from ~6.5 Ma (Solheim et al., 1998; Knies et al., 2009, 2014).

For the area northwest of Svalbard, Mattingsdal et al. (2014) established a seismic correlation using academic and industry seismic data tied to Ocean Drilling Program (ODP)

Leg 151 boreholes. Their results show intensified ocean current development from ~11 to ~2.7 Ma, increased sediment contribution from an ice sheet from ~2.7, and extensive glaciation from ~1.5 Ma in the Yermak Plateau area coinciding with major ice advances in the western Barents Sea (Laberg et al., 2010). These results were supported by Knies et al. (2014) who suggested that pre-glacial uplift was an important precursor for the initiation of the early glaciations in the Svalbard – Barents Sea area. The final glaciation phase occurred after ~1.0 Ma with repeated glaciations of Fennoscandia and the Barents Sea including Svalbard, Franz Josef Land, and Novaya Zemlya (e.g. Svendsen et al., 2004). The southwestern Barents Sea was dominated by large ice streams during glaciations of longer duration separated by more pronounced interglacials from ~0.7 Ma (Laberg et al., 2010).

The understanding of the Cenozoic paleoenvironment of the Arctic Ocean has increased substantially following the International Ocean Drilling Program Arctic Coring Expedition (IODP ACEX) (Moran et al., 2006; Backman & Moran, 2009). The main findings include the middle Eocene glacial influence in the Arctic Ocean (the presence of sea ice) and a major hiatus ranging from 44.4 Ma to 18.2 Ma (St John, 2008; Backman & Moran, 2009). The presence of large icebergs covering the Arctic Ocean is suggested in the Pleistocene (Jokat, 2005). Greenland continental margin appears as the most important source area for sediment accumulation in the Amundsen Basin (Svindland & Vorren, 2002). Kristoffersen et al. (2004) supported this view based on their studies of submarine fan development in the Amundsen Basin.

A significant post-breakup sediment accumulation, with a thickness of up to 7 km is found along the northern Barents Sea continental margin (Vågnes, 1996; Geissler & Jokat, 2004; Engen et al., 2008). However, due to the lack of well data and sparse seismic data coverage, the erosion estimate and the chronology of this margin are poorly constrained. Much of the sediments within the Nansen Basin have likely been supplied from the Barents Sea shelf and adjacent land areas, as the wider Barents Sea has suffered severe erosion in the Cenozoic (e.g. Nyland et al., 1992; Rasmussen & Fjeldskaar, 1996; Henriksen et al., 2011; Laberg et al., 2012; Lasabuda et al., 2018a). A number of methods, both well-based and seismic-based techniques, have been used to quantify uplift and erosion (e.g. apatite fission track, vitrinite reflectance, mass balance, see review by Corcoran & Doré, 2005). The net erosion has been generally estimated of up to 3 km on Svalbard. These Cenozoic uplift and erosion events are suggested to be synchronous along the North East Atlantic margin (Anell et al., 2009; Green & Duddy, 2010), which are related to the early Cenozoic sea-floor opening and late Cenozoic glaciations.

2.3. Continental shelf and slope system in the northern Barents Sea

There are at least eleven trough systems present at the northern Barents Sea continental margin (Batchelor & Dowdeswell, 2014). The major systems are St. Anna, Franz Victoria, and Voronin troughs (Figure 1). The seismic data coverage in the present study only allows analysis on three of them; the Kvitøya, Albertini, and Nordenskjold troughs (Figure 2A). The trough systems are variable in size and dimension, but most of them show a widening trend towards the shelf break. The Kvitøya, Albertini, and Nordenskjold troughs show an upper-slope gradient of 5.5°, 1.7°, and 2.9°, respectively (Batchelor & Dowdeswell, 2014). The dimension and the drainage area of the Kvitøya Trough are larger than Albertini and Nordenskjold troughs. The Nordenskjold Trough (Cherkis et al., 1999) is the westernmost trough system in this study and shows a relatively similar dimension with Albertini Trough. The paleo-ice stream drainage area is also inferred to be similar for both troughs.

Glacial landforms resulting from ice sheet advance and retreat during the last glacial period characterize the northern Barents Sea continental shelf (Dowdeswell et al., 2010a; Hogan et al., 2010; Batchelor et al., 2011; Fransner et al., 2017a). These include megaflutes, drumlins, and iceberg ploughmarks, with various orientations and scales. Based on shallow cores, the lithology of the shelf consists of a range of deposits from clay to sand, diamicton, bioturbated strata, and mud with occasional dropstones (e.g. Kleiber et al., 2000; Batchelor et al., 2011; Fransner et al., 2017b; 2018).

2.4. Seafloor morphology

The bathymetry at the lower slope of the northern Barents Sea continental margin shows an irregular topography with a series of angular features (Figure 3A). These features are interpreted as canyons and gullies resulting from erosion by flows and/or currents from small-scale slope failures remobilizing sediment from the upper slope towards the basin (Figure 3B). The canyon dimensions are up to 20 km in length, 6 km in width, and ~1 km in depth (Figs 3B and C). The width of the gullies are typically from 100 to 500 m with a depth of about 150 m.

The morphology of the canyons includes slide scars, indicating sediment remobilization towards the deep basin (Figure 3C). The dominating processes are inferred to be debris flows and slumps on the upper slope, which may have transformed into partly erosive turbidity currents downslope. Thus, this part of the northern Barents Sea continental margin was dominated by erosion. Some of the areas flanking the canyon or gullies show smooth morphology, which may have been smoothed by contour currents (Figure 3B). In the Nansen Basin, the seafloor has a rough morphology interpreted as megablocks, probably formed as part of the Hinlopen slope failure.

3. Data and methods

Multi-channel seismic data were provided by the Alfred Wegener Institute (AWI), Norwegian Petroleum Directorate (NPD), and Federal Institute for Geosciences and Natural Resources (BGR) (Figure 2A). The multibeam bathymetry data were provided by AWI, and this was acquired in the period of 1998 – 2013, while the seismic data were acquired in the period of 1990 – 2013. The overall quality of the bathymetric and seismic data is good. The seismic interval velocity for depth conversion was derived from Geissler & Jokat (2004). The velocity range is 2.1 – 2.7 km/s for the deeper strata (NB-2; Figure 4), resulting in an average velocity of 2.3 km/s (Geissler & Jokat, 2004). Assuming a dominant frequency of 20 – 50 Hz, the wavelength range is from 40 to 250 m, giving a vertical resolution of ca. 10 m for the shallow and ca. 60 m for the deep strata. The closest wellbores are the ODP sites 910, 911, and 912 at the Yermak Plateau (Figure 2A).

In this study, we aim to separate the glacial and pre-glacial strata (Figure 4). The deposited glacial sediments in the basin are mapped and the corresponding volumes are estimated as an input for the mass balance (source-to-sink) approach. Then, the most likely source area (drainage) is delineated. The volume of the deposited sediments in the basin is assumed to be equal to the eroded sediment in the source area with some corrections (e.g. Laberg et al., 2012; Lasabuda et al., 2018b). The first correction is related to the sedimentary processes involved, as some of the sediments deposited along the continental margin may not be derived from the delineated source area (e.g. the parts comprising contourites). Therefore, these need to be excluded from the deposited sediment volume before converting to the eroded sediment volume. Secondly, correction related to sediment compaction. This study is focused on the uppermost part of the sedimentary succession along the continental margin,

meaning that the source of this succession was probably more compacted due to source area overburden. Lastly, correction related to the bedrock composition is needed if the source area consists of higher density crystalline bedrock (Dowdeswell et al., 2010b).

Another uncertainty is the delineation of the source area. The mass balance method is dependent on the relative size of the source area, which may also vary for each period of glaciation. We consider the glaciation model by Knies et al. (2009) and various LGM ice sheet reconstructions (e.g. Lambeck, 1995,1996; Dowdeswell et al., 2010a; Patton et al., 2015) to better constrain the size of the source area.

4. Results

In this section, the seismic stratigraphy analysis is presented. This includes a seismic facies description based on Mitchum Jr et al. (1977), followed by a description of the seismic units from east to west and from shelf to basin. Subsequently, the seafloor morphology, a revised chronology, and the volumetric mass balance are presented.

4.1. Seismic facies

4.1.1. SF1a: Chaotic

Description–Medium to high amplitude reflections and chaotic internal seismic signature with an irregular base and top characterize this seismic facies (Figure 5).

Interpretation–SF1a is interpreted as deposits from gravity-driven processes (e.g. debrites, slumps, and slides). These deposits are often jointly classified as a mass-transport deposit (MTD). The high amplitude reflections may represent sub-angular/rotated blocks of coarser lithology and/or more compacted deposits (e.g. Alves, 2010). The irregular base indicates an erosive surface.

4.1.2. SF1b: Semi-transparent

Description–Low amplitude discontinuous reflections, and internally semi-transparent to structureless with an irregular base characterize this seismic facies (Figure 5).

Interpretation–SF1b is also interpreted as debrites, and/or deposits from slumping and sliding, jointly categorized as MTDs, but interpreted to be more thoroughly remolded deposits as compared to facies SF1a. An erosive basal surface is indicated by the irregular base.

4.1.3. SF2: Tangential/oblique.

Description–Low to medium amplitude and relatively continuous inclined reflections characterize this seismic facies (Figure 5).

Interpretation–SF2 represents a prograding sediment wedge and is interpreted as a high-gradient TMF following Rydningen et al. (2016). Other terms have previously been used for similar deposits including glacial prograding wedge (Dahlgren et al., 2005), glacial delta (Nielsen et al., 2005), and glacial-sedimentary prism (Batchelor & Dowdeswell, 2014).

4.1.4. SF3: Parallel to sub-parallel.

Description–Low to medium amplitude, continuous to semi-continuous reflections with often conformable top and base characterize this seismic facies (Figure 5).

Interpretation—SF3 represents deposition through hemipelagic processes. This facies is often interpreted as glacimarine sediments in a high-latitude setting resulting from slow sedimentation by iceberg/sea ice including ice-rafted debris (IRD) (e.g. Larsen et al., 1994; King et al., 1996). Similar packages are commonly found at the distal part of TMFs and may represent turbidite sheets/fans of sand-shale interlayers (Laberg & Vorren, 1996; Batchelor & Dowdeswell, 2014; Laberg et al., 2018). This seismic facies can also be interpreted as sediment drifts in the area where contour currents are dominating (e.g. Rebesco et al., 2014).

4.1.5. SF4: Contorted.

Description—Low to high amplitude, semi-continuous reflections, with mounded geometry characterize this seismic facies (Figure 5).

Interpretation—SF4 is interpreted as contourite drifts, which are developed under the influence of ocean currents (Stow & Lovell, 1979). Contourite drifts are typically seen as imbricated asymmetrical sediment layers, representing deposition on one side (often described as elongated and mounded drift) and erosion on to the other (Hernández-Molina et al., 2008). The lithology is typically dominated by mudstone and the higher amplitude in the seismic may be associated with the presence of coarser sediments (Rebesco et al., 2014).

4.2. Seismic units and chronology

The Cenozoic succession of the respective areas of the northwestern Barents Sea continental margin has previously been divided into three seismic units by Geissler & Jokat (2004), i.e. the Nansen Basin (NB) has been divided into NB-1 (oldest), NB-2, and NB-3. A similar naming style has been applied for the area of Kvitøya (KV) and Nordaustlandet (NA).

For simplicity, we unify the naming for KV, NA, and NB into one (NB) as the focus in this study is on the glacial strata, which is then further subdivided into NB-3A, NB-3B, and NB-3C (Figure 6). We also name the upper unit of the pre-glacial strata in Kvitøya, Nordaustlandet, and Nansen Basin as NB-2. A submarine slide, called “Body A” by Engen et al. (2009) in the Nansen Basin is described in more detail in this sub-chapter.

No academic or commercial wells are available from the study area, thus the age of the sediments relies on the age model from ODP drilling in northwest and west of Svalbard. A revised chronology by Knies et al. (2014) for these cores implies that the base of NB-3A is correlated to the base of YP3 in the Yermak Plateau, which is dated to ~2.7 Ma. This age marked the first shelf edge glaciation in the Yermak Plateau and likely in the northern Barents Sea according to Knies et al. (2014). Mattingsdal et al. (2014) reported buried iceberg plough marks indicating a major glacial expansion in the Yermak Plateau at ~1.5 Ma, which is correlated to the base of unit NB-3B. This age slightly revised the ~1.6 Ma age estimate of Butt et al. (2000). The next important glaciations phase is indicated after ~1.0 Ma (Knies et al., 2009), here tentatively set to ~0.7 Ma, corresponding to the base of unit NB-3C. This is following the paleoenvironmental reconstruction for the southwestern Barents Sea part of the Svalbard-Barents Sea Ice Sheet (SBSIS), implying more polar ice conditions from ~0.7 Ma (Laberg et al., 2010).

This age model implies that the sediments of NB-3A was deposited in the period from ~2.7 to ~1.5 Ma, followed by NB-3B from ~1.5 to ~0.7 Ma, and NB-3C for the last ~0.7 Ma (Figure 6). This age model, thus, slightly revises the age model from Geissler & Jokat (2004) and Engen et al. (2009). However, stratigraphically, we have picked the same seismic horizons as these previous works also tied to the ODP sites in the Yermak Plateau.

The exact age at the base of NB-2 is presently not known. As we interpret NB-2 to mainly comprise contouritic sediments, it is here tentatively suggested to comprise sediments

≤ ~17.5 Ma, from which a gradual increase in intensity of the ocean circulation has been inferred (Jakobsson et al., 2007).

4.2.1. Unit NB-2

Description—This unit is dominated by SF3 (Figures 7B and 8) and SF4 (Figures 8, 9, and 10), i.e. a parallel to sub-parallel and contorted internal seismic signature. On the upper slope, NB-2 also includes acoustically chaotic to transparent intervals (SF1b) (Figure 7). There is an increasing amplitude from the base towards the top (e.g. Figure 10). Further downslope, the base of NB-2 is not easy to define as the amplitude of the reflections are generally weak, but an apparent onlapping sequence towards the basement high is observed (Figure 7B). The thickness is up to 1080 m in the proximity of the boundary fault and fairly uniform, ca. 700 m, towards the Nansen Basin (Figures 4 and 9).

Interpretation—The seismic facies analysis indicates predominantly hemipelagic sedimentation and/or contouritic deposits suggesting that this unit was influenced by ocean currents. On the upper slope, the occurrence of facies SF1b indicates that mass-wasting processes have affected the unit NB-2 deposits. The contact between NB-2 and the basement high is likely an erosional surface considering the onlapping stratal pattern.

4.2.2. Sub-unit NB-3A

Description—NB-3A is dominated by SF2 (tangential/oblique facies) above a prominent unconformity truncating underlying reflections below the Kvitøya TMF (Figure 7B) and in front of the Albertini Trough (Figure 8). At least six major bedsets are observed in this sub-unit forming the lower part of the Kvitøya TMF (Figure 7B). SF3 and SF4 dominate to the west along the continental slope (e.g. Figures 8, 9, and 10). In the Nordenskjold Trough, NB-3A rests conformably on NB-2. A prominent truncation of SF3 is observed west of the Nordenskjold Trough, and sediments dominated by SF1 rests on this unconformity. In the Nansen Basin, SF1a (e.g. Figure 8) and SF1b (Figure 11) dominates. The thickness of this unit is up to 740 m (Figure 12A) in the Kvitøya TMF. The isopach map shows sediment thinning towards the upper shelf and locally in the proximity of seamounts (Figure 12A).

Interpretation—The prominent clinofolds in the Kvitøya and Albertini TMFs are interpreted as stacked glaciogenic debrites, recording repeated advances of grounded ice sheets to the shelf break. The sediment input was most pronounced through the Kvitøya Trough. At the mouth of the Nordenskjold Trough, this influence was less pronounced, instead the seismic facies indicate contourite drifts, hemipelagic and/or glacimarine deposit. NB-3A is here locally including headwall failures, indicating instability of NB-3A (Figure 10A). West of the Nordenskjold Trough, sediment waves occur, suggesting that ocean currents dominated here (Figure 10B). In the Nansen Basin, the Body A is stratigraphically located within NB-3A and shows an erosive base (Figure 11B). A series of rotated blocks are interpreted in the proximal part of the body (Figure 11B). From our dataset, it is now possible to better constrain the western extent of this slide deposit (Figure 11C). However, the eastern extent of this body remains uncertain due to limited seismic data coverage.

4.2.3. Sub-unit NB-3B

Description— NB-3B predominantly comprise facies SF2 (tangential/oblique) on the upper continental slope across the Kvitøya Trough. Here, NB-3B shows more steeply dipping and discontinuous reflections as compared to the underlying sub-unit (Figure 7). At the mouth of the Albertini Trough, the internal reflections of SF2 are more continuous and steeply dipping compared to the underlying sub-unit (Figure 8). The NB-3B of the Kvitøya

Trough shows at least eight densely spaced bedsets (Figure 7A). SF3 and SF4 still dominate further to the west along the continental slope at the Nordenskjold Trough (Figures 9 and 10). In the Nansen Basin, NB-3B is dominated by SF1a and SF1b (Figure 11B). Here, this sub-unit subcrops the bathymetry. The thickness of NB-3B is up to 500 m in the footwall of to the boundary fault. The major depocenters include the Kvitøya TMF to the Nansen Basin (Figure 12B).

Interpretation—The seismic facies analysis suggests a high-gradient TMF in the outer parts of the Kvitøya and Albertini troughs. The sediment input was still most distinct in the Kvitøya Trough, but less so in the Albertini Trough. An unconformity separates NB-3A and NB-3B in the Albertini Trough, but this is less obvious in the Kvitøya Trough (Figures 7 and 8). The seismic facies composition suggests sheeted drifts, hemipelagic and/or glacial-marine deposits as well as debris lobes in the Nordenskjold Trough (Figure 9). No obvious high-gradient TMF developed in this trough (Figure 9). Seismic data indicate that this area still was influenced by along-slope flowing ocean currents (Figure 10B). In the Nansen Basin, NB-3B contains predominantly stacked glacial-marine debris lobes (Figure 11B).

4.2.4. Sub-unit NB-3C

Description—NB-3C is dominated by SF1 and SF3 at the shelf, and SF2 in the upper slope of Kvitøya and Albertini troughs (Figures 7 and 8). Here, it appears as an aggradational unit with an irregular upper boundary. NB-3C is thin or even absent in the Nordenskjold Trough (Figure 9). Towards the Nansen Basin, this sub-unit wedges out (Figure 12C). The thickness is up to 170 m at the shelf break and shows limited distribution basinwards (Figure 12C).

Interpretation—The seismic facies composition suggests that NB-3C is dominated by debrites (Figures 7 and 8). In the Kvitøya and Albertini troughs, the morphology of NB-3C is interpreted to be formed by subglacial till affected by iceberg ploughing, which can be followed to the continental slope (Figures 7 and 8). At the Kvitøya TMF, NB-3C forms the topset and the outermost part of the foreset of the glacial-sedimentary strata and thins out downslope. (Figure 7A). Downslope of the Albertini Trough, an irregular slope morphology is attributed to a slump deposit (Figure 8).

4.3. Volumetric mass balance

The isopach maps show the total sediment volume and its distribution. The corresponding volumes are used to calculate the average sedimentation rates and from this, average erosion rates in the source area are estimated. A few corrections are applied, as detailed in the mass balance flowchart by Lasabuda et al. (2018b).

4.3.1. Depositional volume, area, and sedimentation rates

The total volume of Plio–Pleistocene sediments is estimated to be 29,000 km³, which gives an average sedimentation rate of about 0.24 m/Kyr over the last ~2.7 Ma (Table 1). The estimated sedimentation rates for NB-3A and NB-3B are ca. 0.2 m/Kyr and ca. 0.77 m/Kyr, respectively. The size of the depositional area is up to ~44,000 km² (Table 1). A lower sedimentation rate of about 0.12 m/Kyr is found for the period corresponding to NB-3C (Table 1). Body A is excluded from these calculations; this volume is estimated to be ~6700 km³, and covers an area of ca. 27,000 km².

4.3.2. Volume correction due to deposition of contourites

Our seismic mapping shows that NB-3A appears to contain contourites on the upper slope outside and between the areas in front of the shelf troughs (Figures 7 – 10). A large portion of contourites consist of sediment deposits commonly fed by down-slope sediment processes i.e. turbidity currents, which have a local provenance (e.g. Stow et al., 2008). Contour currents may also bring sediments from outside the considered source area and these sediments need to be excluded from the sediment budget calculations before converting to erosional volume. Thus, we tentatively applied a 10% reduction to the NB-3A volume, reducing it from ~11,000 to ~10,000 km³ before other corrections are applied (Table 2).

We also excluded the western part of the Franz Victoria TMF from our sediment budgeting as these deposits were mainly sourced from outside the considered drainage area (Figure 11A). The bathymetry data shows a pronounced outward bulge of the continental rise off the Franz Victoria Trough (Figure 2A) comprising glacial debris lobes. This stack of glacial debris lobes is interpreted to be part of the Franz Victoria TMF (Figure 11B). A similar spatial correction is applied to exclude deposits of the Hinlopen Slide.

4.3.3. Drainage area delineation

For the source area, we have considered a minimum and maximum alternative (Figure 12D). The minimum source area is based on the LGM ice divides south of the Hinlopen Trough and over Nordaustlandet (Dowdeswell et al., 2010a; Hogan et al., 2010; Hormes et al., 2011; Patton et al., 2015; Figure 12D). The maximum estimate of the source area is based on LGM ice divides over Storbanken, southeast of Kong Karls Land (Lambeck, 1995, 1996; Ottesen et al., 2005; Patton et al., 2015; Figure 12D). We also consider lateral ice sheet extent for each glaciation (Svendsen et al., 2004; Knies et al., 2009) as we will discuss below.

The minimum source area is considered similar for all seismic units, which corresponds to ~32,000 km² (Table 2). The maximum source area is also identical for all units (~63,000 km²), except for NB-3A, which is estimated to be ~49,000 km² (Table 2). This difference is due to the ice coverage during the period of deposition of NB-3A, which is inferred to be rather small (Knies et al., 2009; Figure 12A).

4.3.4. Volume correction due to compaction and bedrock composition

It is more likely that the rocks in the source area with the highest porosity were eroded first, i.e. in the early Cenozoic. Then the rocks eroded later in the late Cenozoic, had the deepest burial and the lowest porosity (highly compacted). Therefore, the depositional volume of the upper Cenozoic strata will likely be more than their erosional volume. From Figure 4, the lowest base of the pre-glacial strata are at ~7 km and the depth of glacial strata are at average of ~4 km. This means ~3 km overburden for the lowest pre-glacial strata. Based on porosity-effective stress diagram (Bjørlykke et al., 2015), a ~3 km overburden would give about 5% decompaction factor for a fine-grained sediments (e.g. Lasabuda et al., 2018a). Similarly, the depositional volume of glacial strata need to be subtracted by 5% compaction factor in order to estimate the erosional volume.

The last correction is related to bedrock lithology differences. The minimum drainage area includes the northern part of Nordauslandet that is dominated by Precambrian bedrock including intrusive rocks as well as gneisses, amphibolites, and migmatites (Dallmann, 2015). To compensate for a higher density of the crystalline bedrock (~2.7 g/cm³) compared to sedimentary rocks in the basin (~2.2 g/cm³), we applied a correction of 20% (i.e. the considered bedrock volume was 20% lower) (Table 2) in accordance with Dowdeswell et al. (2010b).

For the maximum drainage area, we tentatively applied half of the correction (10%), as this alternative includes a larger shelf area composed of sedimentary rocks of Mesozoic age (Dallmann, 2015; Table 3). These corrections give values ranging from ~21,000 to ~24,000 km³ for the total volume of the eroded bedrock during the Plio–Pleistocene (Table 2).

4.3.5. Sediment discharge, sediment yield, net average erosion, and average erosion rates

Assuming a sediment density of 2.2 g/cm³, we estimate a sediment discharge of 17 – 20 x 10⁶ t/yr (Table 2). Sediment yield estimates are in the range of 310 – 540 t/km²/yr. The average net erosion is calculated to be 410 – 650 m with average rates of erosion of 0.15 – 0.24 m/Kyr (Table 2). The average net erosion appears to be the highest for the NB-3B period (~1.5 – ~0.7 Ma) and the lowest in the NB-3C period (< ~0.7 Ma) (Table 2).

5. Discussion

5.1. Late Cenozoic paleoenvironmental reconstruction

5.1.1. Period from ~17.5 to ~2.7 Ma (NB-2)

Our seismic stratigraphic and facies analysis show that marine hemipelagic/glacimarine and contouritic sediments dominated the continental margin succession from ~17.5 to ~2.7 Ma. Contour currents appear as the dominant processes as seen from the amount of contourites deposited at the shelf and upper slope (Figure 13A). Sediment supply from onshore and/or the shelf towards the shelf break may have been relatively small. On the lower slope and in the Nansen Basin, hemipelagic/glacimarine and mass-wasting processes controlled the sediment transport and deposition.

A similar observation of contourites has been presented for the Yermak Plateau (Geissler et al., 2011) and the Fram Strait area (Gebhardt et al., 2014) further west, signifying the importance of the contour currents for the development of the northwestern Barents Sea sector of the Arctic Ocean. The opening of the Fram Strait connecting the northern North Atlantic and the Arctic Ocean (Kristoffersen, 1990; Engen et al., 2008) initialized the ocean current system responsible for this sedimentation pattern. This opening, which significantly contributed to deep-water exchange through the Fram Strait and oxygenating the Arctic Ocean, is interpreted to have occurred from ~17.5 Ma after which the Arctic Ocean was no longer a land-locked basin (Jakobsson et al., 2007).

Onlap of unit NB-2 onto the basement suggest that northeastern Svalbard was likely a positive morphological feature some time before the Miocene (Figures 14A and B). The upper Miocene strata in the Albertini Trough are truncated, indicating a hiatus in the late Miocene (Figure 14C), before the deposition of the glacial wedge (Figure 14D). This observation may suggest a pre-glacial uplift, possibly a rift-flank uplift. Similar observation has been reported in the southwestern Barents Sea (Lasabuda et al., 2018a). This is in agreement with the regional exhumation pattern along the margin of the North East Atlantic realm (Anell et al., 2009; Green & Duddy, 2010). These uplift and erosion events may have been controlling the initial location of the small-scale glaciations that likely affected Svalbard and its northeastern continental margin (Knies & Gaina, 2008; Knies et al., 2014; Figure 15A).

In the Arctic Ocean, the earliest NB-2 deposition probably marks the onset of sedimentation following a major hiatus (44.4 Ma – 18.2 Ma) interpreted from a drill core at the Lomonosov Ridge (Moran et al., 2006). The ACEX cores show the presence of IRD in

the deposits younger than 18.2 Ma indicating glacial marine sediment deposition from icebergs (Backman & Moran, 2009).

5.1.2. Period from ~2.7 to ~1.5 Ma (NB-3A)

The deposition of NB-3A reflects the first period of repeated large-scale coastline-shelf edge glaciations. The Kvitøya TMF shows the most intense progradation, suggesting the presence of fast-flowing ice streams feeding this TMF (Figure 13C). Whereas, the Nordenskjold TMF appears to be less-developed indicating that this TMF was fed from a slower-moving (a more sluggish) ice sheet. Moreover, a substantial increase in sediment drift deposition is observed in front of the trough. This observation indicates a still important role of sedimentation from contour currents in shaping the continental margin in the western part.

In the early development of the Kvitøya TMF, a large slope failure event resulted in the deposition of Body A, transferring a large volume of contouritic and hemipelagic/glacial marine sediments into the Nansen Basin (Figure 13B). This event is probably occurred slightly prior to ~2.7 Ma based on the seismic stratigraphic position of Body A (see Figure 4).

The ice sheet extent and thereby the ice drainage have varied over the late Pliocene period. From ~3.5 to 2.4 Ma, ice extent may have been limited in the Barents Sea (Knies et al., 2009; Figure 12A) with first shelf edge glaciations occurred at ~2.7 Ma (Knies et al., 2014). Globally, a dynamic transition from regionally restricted to more large-scale glaciations occurred as a result of a complex interaction of tectonic, climatic, and paleoceanographic factors (Mudelsee & Raymo, 2005; Matthiessen et al., 2009). In the Nordic Seas, a continuous ~3.5 Ma old IRD record has been reported from ODP site 907 offshore Greenland and expansions of Greenland glaciers has been interpreted from ~3.3 Ma (Jansen et al., 2000; Kleiven et al., 2002).

5.1.3. Period from ~1.5 to ~0.7 Ma (NB-3B)

Repeated advances of an ice stream towards the paleo-shelf break likely occurred in the Kvitøya Trough (Figure 13D). There were also ice streams in the Albertini and Nordenskjold troughs, although they may have been smaller compared to the Kvitøya ice streams. In the Nansen Basin, MTDs dominate the succession. Glacial marine and hemipelagic deposits are also present in the Arctic Ocean indicating the presence and absence of sea ice, respectively (Jakobsson et al., 2014).

The IRD record from offshore western Svalbard shows a glacial intensification occurred at ~1.5 Ma (Fronval & Jansen, 1996). From this time onwards, a more regional shelf progradation is observed in front of many troughs in the polar region, testifying to the importance of sediment erosion, transportation, and deposition from fast-flowing ice streams (e.g. Dahlgren et al., 2005). During deposition of NB-3B, expanded ice sheets development is inferred in the Barents Sea (Knies et al., 2009; Figure 12B). A seismic section from the Fram Strait, tied to the ODP 910, 911, and 912 boreholes shows evidence of iceberg ploughmarks indicating ice advance reaching the shelf break at ~1.5 Ma but the area of origin of these icebergs is presently not known (Mattingsdal et al., 2014).

5.1.4. Period after ~0.7 Ma (NB-3C)

The erosion surface at the base of NB-3C (Figure 13E), which is particularly well developed within the Kvitøya TMF, may reflect erosion from an expanded shelf edge glaciation in the northern Barents Sea area. A comparable erosional surface is termed the

Upper Regional Unconformity (URU) in the western Barents Sea (e.g. Vorren et al., 1991) or Glacial Unconformity (GU) in the UK margin (Stoker et al., 2005). Nielsen et al. (2005) indicated that this surface varies in age across the polar region. They suggested that URU and the change in sediment depositional style from progradation to aggradation might represent a change in the ice sheet extent. The preserved topset of the TMF may also be due to, in part, increasing subsidence due to loading-unloading processes (Dahlgren et al., 2005).

A series of canyons at the lower slope of the Nordenskjold Trough indicate that smaller scale slope failure events dominated. In addition, gullies, channels, and sediment lobes are documented from the Albertini and Kvitøya troughs by Fransner et al. (2017a; 2018) that is in agreement with slope instability. Some parts of the canyons are relatively smooth, which may indicate the deposition by contour currents. In the eastern part of the Hinlopen scar, Geissler et al. (2016) also suggested sediment wave development. This suggestion fits well with results from this study that indicate a western increase in the influence of contour currents (Figure 15B).

Expanded glaciations have been reported from many parts of the North Atlantic realm during the last 1 Ma (see Dahlgren et al., 2005), as seen from major increases of IRD content that reflect the extent and magnitude of ice sheets (e.g. Mangerud et al., 1996). The NB-3C was deposited during these periods of the largest ice sheet extent (Knies et al., 2009; Figure 12C).

5.2. Controlling factors of the trough-mouth fan development

A number of factors, ranging from the size and bedrock types of the drainage area, ice dynamics, and continental slope gradient, likely controlled the sedimentary succession and its variation across the study area.

The bedrock substrate appears to influence the amount of eroded sediments and directly affects the sediment volume transported basinwards. An area consisting of sedimentary rocks (e.g. central and western Barents Sea shelf) is more prone to glacial erosion than a source area comprising crystalline bedrock (e.g. mainland Svalbard) (Table 3). The bedrock composition of the drainage area feeding the Kvitøya TMF is relatively 'soft' (dominated by sedimentary rocks) compared to the drainage area of the Nordenskjold and the Albertini troughs that composed of predominantly crystalline bedrock (Dallmann, 2015). This hypothesis can, at least partly, explain the major sedimentary thickness increase in front of the Kvitøya Trough (Figure 12B).

The dynamics of the SBSIS, including the location of the ice divides controlling the ice drainage area and ice flow, also appears to be controlling the size of TMFs. Although the ice drainage during the late Quaternary in the Barents Sea area is reasonably well defined based on the present-day bathymetry (e.g. Landvik et al., 1998; Minakov et al., 2012), the locations of the main ice divides are still debated (Dowdeswell et al., 2010a; Patton et al., 2015). The position of ice divides is an important factor in determining the relative amount of ice draining the area and thus the volume of sediments deposited along the margin. This is confirmed by ice sheet modeling showing that the Bjørnøya TMF received sediment from a significant portion of the Barents Sea shelf during the last glaciation (Patton et al., 2015). A considerably smaller catchment area has been inferred for the Troms margin TMFs, a likely analogue to the setting northeast of Svalbard, resulting in a much smaller volume of sediments along this part of the margin (Rydningen et al., 2016).

Furthermore, the basal temperature conditions may have influenced the effectiveness in eroding the substrate implying cold-based ice is less erosive in contrast to warm-based ice (Elverhøi et al., 1998; Bierman et al., 2016). Therefore, in contrast to the Kvitøya Trough, we

suggest that the Nordenskjold Trough may have been occupied by colder-based ice delivering significantly less sediments off the margin.

Relatively lower sediment accumulation is found off the Kvitøya, Albertini, and Nordenskjold troughs compared to the western Barents Sea. Their TMF styles are also different compared to the Bjørnøya or Storfjorden TMF. The Kvitøya TMF is comparable in size and morphology to TMFs located along the Troms margin (Rydningen et al., 2016) and southeastern Greenland (Larsen et al., 1994). Slope gradient of the receiving basin seems to play a role in controlling the presence, geometry, and dominating deposits of TMFs. Steeper gradients often result in high-gradient TMFs or glacial-sedimentary prisms (e.g. Troms margin TMF). Batchelor & Dowdeswell (2014) suggested that a steep slope-gradient ($>4^\circ$) is likely to prevent major/giant TMF development (e.g. Bjørnøya TMF), which fits our observation.

Fransner et al. (2017a) suggested that faulting in the underlying basement was the primary cause for the less developed Albertini TMF. This contradicts our finding, which shows no obvious fault growth penetrated the glacial strata, indicating that the down faulted topography had likely little or no influence in controlling the deposition of glacial sediments in this trough (Figure 14). To the west, in the Nordenskjold Trough, however, fault growth may have influenced the development of sediment drifts (Figure 9A). This observation may be attributed to slope instability due to abundance of contourites that are prone to slope failure (e.g. Geissler et al., 2016; Elger et al., 2017).

5.3. Late Cenozoic average sedimentation rates, net erosion estimates, and erosion rates – A comparison

The estimated average sedimentation rate for NB-3A to NB-3C over the last ~2.7 Ma is 0.24 m/Kyr. A comparable number, 0.17 m/Kyr, was previously reported for the last ~2.6 Ma (Geissler & Jokat, 2004). We detailed this interval and found a trend of increasing sedimentation rates from the period of NB-3A (0.2 m/Kyr) to NB-3B (0.77 m/Kyr). Although using a different age model, a similar increasing trend was also reported by Engen et al. (2009), from 0.27 m/Kyr for their NB-4A to 0.3 m/Kyr for their NB-4B. From the Troms margin offshore northern Norway, a mass balance study of the glacial succession showed an average sedimentation rate of 0.15 – 0.22 m/Kyr (Rydningen et al., 2016), i.e. very similar to our numbers (Table 3).

Our sedimentation rate of NB-3B (0.77 m/Kyr) for the period of ~1.5 – ~0.7 Ma is in agreement with 0.63 m/Kyr sedimentation rates from the Storfjorden TMF in the northwestern Barents Sea (Hjelstuen et al., 1996). Moreover, comparable sedimentation rates have also been documented from the southwestern Barents Sea margin showing sedimentation rates varying between 0.22 and 0.64 m/Kyr for the Quaternary GI–GIII units (Faleide et al., 1996; Laberg et al., 2012). On the Yermak Plateau, average sedimentation rates for the last 1 Ma at the three ODP sites 910, 911, and 912 are up to 0.1 m/Kyr (Mattingsdal et al., 2014). This value is in agreement with our estimate for NB-3C, 0.12 m/Kyr.

Our numbers reflect the rate of sediment contribution towards the Arctic Ocean from the northwestern Barents Sea shelf. Levitan (2015) compiled a map of sedimentation rates for the Arctic showing that the study area has an average sedimentation rate of >0.03 m/Kyr for the last 130 ka. Our numbers (0.12 m/Kyr) for the last ~0.7 Ma fit with this, which correspond to the general pattern of average sedimentation rates for the Arctic Ocean.

For the first time, average net erosion and erosion rates are estimated for the drainage area of the studied margin, showing an average erosion of 410 – 650 m. In comparison, the late Cenozoic (glacial) erosion estimates from the western Barents Sea margin have been

reported to be 1100 m and 1700 m for the southwestern (Laberg et al., 2012) and northwestern margin (Hjelstuen et al., 1996), respectively (Table 3). These results show that the western margin of the Barents Sea experienced more severe glacial erosion as compared to its northern segment.

It has been suggested that half to two thirds of the deposits of the major TMFs along the western Barents Sea margin were of glacial origin (Fiedler & Faleide, 1996; Hjelstuen et al., 1996; Minakov et al., 2012). In contrast, the glacial to non-glacial ratio of the northeastern Svalbard margin seems to be lower based on our observations. This is likely because the major glacial drainage pattern is towards the western Barents Sea (Bjørnøya Trough). However, prominent trough systems are also present along the northern margin (Franz Victoria and St. Anna troughs) suggesting high glacial erosion east of the study area.

Although similar in progradation style, our erosion rate is significantly higher than the average rate of erosion of Troms margin TMF (Table 3). This discrepancy may be due to the location of the Troms TMF in between two major ice sheets, the SBSIS and Fennoscandia Ice Sheet (Rydningen et al., 2016). Our maximum erosion rate (0.24 m/Kyr) is comparable with the 0.19 m/Kyr. reported from the mid-Norwegian margin (Dowdeswell et al., 2010b) and the 0.2 m/Kyr calculated for the western Svalbard margin (Elverhøi et al., 1998) (Table 3). These similarities can partly be attributed to a similar bedrock composition in the drainage areas (Elverhøi et al., 1998).

5.4. The Body A compared to other slides along the Norwegian continental margin

In terms of size (i.e. area affected), the Body A slide is smaller compared to the mega slide deposits from the southwestern margin of the Barents Sea (Hjelstuen et al., 2007) (Figure 16). The volume of sediments involved is comparable to the northwestern Barents Slide reaching a volume of 4100 km³ (Safronova et al., 2015). The Body A is approximately double the size of the Holocene Storegga Slide offshore mid-Norway (Haflidason et al., 2004), but interestingly only less than half in terms of area affected. The reason for this is presently not known. Assuming that our age estimate is correct (at about ~2.7 Ma), Body A is likely to be one of the oldest described slides along the Norwegian continental margin.

The underlying unit (NB-2) which is dominated by contourites, may precondition the development of glide planes for a submarine slope failure. There are several possible triggering mechanism for Body A. The slope failure may have occurred due to the initial loading of the pre-glacial margin by subglacially derived debris flows. This mechanism has been observed elsewhere in high-latitude margins, including the Antarctic margin (Rebesco & Camerlenghi, 2008). Another alternative is seismicity, a similar mechanism as the neighboring Hinlopen Slide (Vanneste et al., 2006). Possible tectonic uplift prior to glaciations may also be contributed to the initiation of such failure (Figure 14C). The interplay of these factors reflects the slope instability of the northern Barents Sea margin.

6. Conclusions

- Analysis of multi-channel seismic data reveal the Neogene – Quaternary paleoenvironmental development of the northeastern Svalbard – northern Barents Sea margin in the area of the Kvitøya, Albertini, and Nordenskjold troughs.
- The period from ~17.5 to ~2.7 Ma was characterized by intensified contour current development related to the opening of the Fram Strait. The deposited succession shows very little or missing influence from ice sheets. Ice advances to the shelf break delivering glacial debris dominated the subsequent period from ~2.7 to ~1.5 Ma, while inter-trough areas were dominated by contourite deposition. The following

period, from ~1.5 to ~0.7 Ma, marked more expansive glaciations. Glacigenic debrites still dominated the succession off the Kvitøya and Albertini troughs. Finally, the period after ~0.7 Ma was characterized by the deposition of overall aggrading packages of the glacial-sedimentary wedges indicating the final advancing of the ice streams particularly in the Kvitøya TMF.

- The lateral variation and temporal evolution of the margin show predominantly mass-wasting processes to the east and contour current processes towards the west. This variation is interpreted due to the size and bedrock types of the drainage area, ice dynamics, and the continental slope gradient.
- The total sediment volume for the studied segment of the margin in the period from ~2.7 Ma to recent is ca. 29,000 km³, giving an average sedimentation rate of 0.24 m/Kyr. This rate is of the same order of magnitude as other glaciated margins, including the western Svalbard and mid-Norway margins, but ~50% less than for the western Barents Sea margin.
- The average net erosion is estimated to be 410 – 650 m, affecting a drainage area of 32,000 – 63,000 km², which covers the studied troughs and the northern part of Nordaustlandet with average erosion rates of 0.15 – 0.24 m/Kyr for the glacial period. Based on our results, the northeastern Nordaustlandet (both land and shelf) and the area of Kvitøya have been subjected to glacial erosion delivering sediments to the Nansen Basin.
- Body A is a large submarine slide with volume of ca. 6700 km³ covering an area of at least 27,000 km². The pronounced unconformity underneath the Kvitøya TMF on the upper slope could be the potential source area of the Body A. If correct, this slide likely occurred prior to or at the onset of the glaciation in this margin.

Acknowledgments

We are grateful to the Research Council of Norway (grant number 228107) together with academic and industry partners for funding this study through Research Centre for Arctic Petroleum Exploration (ARCEX). Part of the study was supported by the American Association of Petroleum Geologists (AAPG) Foundation Grants-in-Aid Program 2018. We thank the Alfred Wegener Institute Helmholtz Centre for Polar and Marine Research (www.awi.de), the Norwegian Petroleum Directorate (www.npd.no), and the German Federal Institute for Geosciences and Natural Resources Hannover (www.bgr.bund.de) for providing the seismic data. The readers can contact these institutions for a permission to access the seismic data. Schlumberger is acknowledged for the software under the educational license agreement for Department of Geosciences, UiT – The Arctic University of Norway. Helen Dulfer and Laura Swinkels are kindly thanked for proofreading the manuscript. Helpful comments from Edward L. King and discussions with Rune Mattingsdal are much appreciated. We are thankful to Jochen Knies and an anonymous reviewer for providing constructive reviews.

References

- Alves, T. M. (2010). 3D Seismic examples of differential compaction in mass-transport deposits and their effect on post-failure strata. *Marine Geology*, 271(3-4), 212-224. doi:10.1016/j.margeo.2010.02.014
- Andreassen, K., Laberg, J. S., & Vorren, T. O. (2008). Seafloor geomorphology of the SW Barents Sea and its glaci-dynamic implications. *Geomorphology*, 97(1), 157-177. doi:10.1016/j.geomorph.2007.02.050
- Anell, I., Thybo, H., & Artemieva, I. (2009). Cenozoic uplift and subsidence in the North Atlantic region: Geological evidence revisited. *Tectonophysics*, 474(1), 78-105. doi:10.1016/j.tecto.2009.04.006
- Backman, J., & Moran, K. (2009). Expanding the Cenozoic paleoceanographic record in the central Arctic Ocean: IODP Expedition 302 synthesis. *Open Geosciences*, 1(2), 157-175. DOI: 10.2478/v10085-009-0015-6
- Batchelor, C., & Dowdeswell, J. (2014). The physiography of High Arctic cross-shelf troughs. *Quaternary Science Reviews*, 92, 68-96. <http://dx.doi.org/10.1016/j.quascirev.2013.05.025>
- Batchelor, C., Dowdeswell, J., & Hogan, K. (2011). Late Quaternary ice flow and sediment delivery through Hinlopen Trough, Northern Svalbard margin: submarine landforms and depositional fan. *Marine Geology*, 284(1), 13-27. doi:10.1016/j.margeo.2011.03.005
- Batchelor, C., Dowdeswell, J., & Pietras, J. (2013). Seismic stratigraphy, sedimentary architecture and palaeo-glaciology of the Mackenzie Trough: evidence for two Quaternary ice advances and limited fan development on the western Canadian Beaufort Sea margin. *Quaternary Science Reviews*, 65, 73-87. <http://dx.doi.org/10.1016/j.quascirev.2013.01.021>
- Berglar, K., Franke, D., Lutz, R., Schreckenberger, B., & Damm, V. (2016). Initial opening of the Eurasian Basin, Arctic Ocean. *Frontiers in Earth Science*, 4, 91. doi: 10.3389/feart.2016.00091
- Bierman, P. R., Shakun, J. D., Corbett, L. B., Zimmerman, S. R., & Rood, D. H. (2016). A persistent and dynamic East Greenland Ice Sheet over the past 7.5 million years. *Nature*, 540(7632), 256. doi:10.1038/nature20147
- Bjørlykke, K., Høeg, K., & Mondol, N. H. (2015). Introduction to Geomechanics: stress and strain in sedimentary basins, in *Petroleum Geoscience*. edited, pp. 301-318, Springer,
- Brozena, J., Childers, V., Lawver, L., Gahagan, L., Forsberg, R., Faleide, J., & Eldholm, O. (2003). New aerogeophysical study of the Eurasia Basin and Lomonosov Ridge: Implications for basin development. *Geology*, 31(9), 825-828.
- Butt, F., Elverhøi, A., Solheim, A., & Forsberg, C. (2000). Deciphering Late Cenozoic development of the western Svalbard Margin from ODP Site 986 results. *Marine Geology*, 169(3-4), 373-390.
- Canals, M., Lastras, G., Urgeles, R., Casamor, J., Mienert, J., Cattaneo, A., De Batist, M., Haflidason, H., Imbo, Y., & Laberg, J. (2004). Slope failure dynamics and impacts from seafloor and shallow sub-seafloor geophysical data: case studies from the COSTA project. *Marine Geology*, 213(1), 9-72. doi:10.1016/j.margeo.2004.10.001
- Cherkis, N., Max, M., Vogt, P., Crane, K., Midthassel, A., & Sundvor, E. (1999). Large-scale mass wasting on the north Spitsbergen continental margin, Arctic Ocean. *Geo-Marine Letters*, 19(1-2), 131-142.
- Cohen, K., Finney, S., Gibbard, P., & Fan, J.-X. (2016). The ICS international chronostratigraphic chart. *Episodes*, 36(3), 199-204.
- Corcoran, D., & Doré, A. (2005). A review of techniques for the estimation of magnitude and timing of exhumation in offshore basins. *Earth-Science Reviews*, 72(3-4), 129-168. doi:10.1016/j.earscirev.2005.05.003
- Dahlgren, K. T., Vorren, T. O., Stoker, M. S., Nielsen, T., Nygård, A., & Sejrup, H. P. (2005). Late Cenozoic prograding wedges on the NW European continental margin: their formation and relationship to tectonics and climate. *Marine and Petroleum Geology*, 22(9), 1089-1110. doi:10.1016/j.marpetgeo.2004.12.008
- Dallmann, W. K. e. (2015). *Geoscience Atlas of Svalbard*, Norsk Polarinstittutt Rapportserie 148,
- Dowdeswell, J., Ottesen, D., Evans, J., Cofaigh, C. Ó., & Anderson, J. (2008). Submarine glacial landforms and rates of ice-stream collapse. *Geology*, 36(10), 819-822. doi: 10.1130/G24808A
- Dowdeswell, J. A., Canals, M., Jakobsson, M., Todd, B., Dowdeswell, E. K., & Hogan, K. (2016). The variety and distribution of submarine glacial landforms and implications for ice-sheet reconstruction. *Geological Society, London, Memoirs*, 46(1), 519-552. <http://doi.org/10.1144/M46.183>
- Dowdeswell, J. A., & Cofaigh, C. Ó. (2002). Glacier-influenced sedimentation on high-latitude continental margins: introduction and overview. *Geological Society, London, Special Publications*, 203(1), 1-9.
- Dowdeswell, J. A., Hogan, K., Evans, J., Noormets, R., Ó Cofaigh, C., & Ottesen, D. (2010a). Past ice-sheet flow east of Svalbard inferred from streamlined subglacial landforms. *Geology*, 38(2), 163-166. doi: 10.1130/G30621.1
- Dowdeswell, J. A., Ottesen, D., & Rise, L. (2010b). Rates of sediment delivery from the Fennoscandian Ice Sheet through an ice age. *Geology*, 38(1), 3-6. <https://doi.org/10.1130/G25523.1>

- Eiken, O., & Hinz, K. (1993). Contourites in the Fram Strait. *Sedimentary Geology*, 82(1-4), 15-32.
- Elger, J., Berndt, C., Krastel, S., Piper, D. J., Gross, F., & Geissler, W. H. (2017). Chronology of the Fram Slide Complex offshore NW Svalbard and its implications for local and regional slope stability. *Marine Geology*, 393, 141-155. <http://dx.doi.org/10.1016/j.margeo.2016.11.003>
- Elverhøi, A., Hooke, R. L., & Solheim, A. (1998). Late Cenozoic erosion and sediment yield from the Svalbard–Barents Sea region: Implications for understanding erosion of glacierized basins. *Quaternary Science Reviews*, 17(1), 209-241.
- Engen, Ø., Faleide, J. I., & Dyreng, T. K. (2008). Opening of the Fram Strait gateway: A review of plate tectonic constraints. *Tectonophysics*, 450(1), 51-69.
- Engen, Ø., Gjengedal, J. A., Faleide, J. I., Kristoffersen, Y., & Eldholm, O. (2009). Seismic stratigraphy and sediment thickness of the Nansen Basin, Arctic Ocean. *Geophysical Journal International*, 176(3), 805-821. doi: 10.1111/j.1365-246X.2008.04028.x
- Faleide, J. I., Solheim, A., Fiedler, A., Hjelstuen, B. O., Andersen, E. S., & Vanneste, K. (1996). Late Cenozoic evolution of the western Barents Sea-Svalbard continental margin. *Global and Planetary Change*, 12(1), 53-74.
- Fiedler, A., & Faleide, J. I. (1996). Cenozoic sedimentation along the southwestern Barents Sea margin in relation to uplift and erosion of the shelf. *Global and Planetary Change*, 12(1), 75-93.
- Fransner, O., Noormets, R., Chauhan, T., O'Regan, M., & Jakobsson, M. (2018). Late Weichselian ice stream configuration and dynamics in Albertini Trough, northern Svalbard margin. *arktos*, 4(1), 1. <https://doi.org/10.1007/s41063-017-0035-6>
- Fransner, O., Noormets, R., Flink, A., Hogan, K., & Dowdeswell, J. (2017a). Sedimentary processes on the continental slope off Kvitøya and Albertini troughs north of Nordaustlandet, Svalbard–The importance of structural-geological setting in trough-mouth fan development. *Marine Geology*. <http://dx.doi.org/10.1016/j.margeo.2017.10.008>
- Fransner, O., Noormets, R., Flink, A., Hogan, K., O'Regan, M., & Jakobsson, M. (2017b). Glacial landforms and their implications for glacier dynamics in Rijpfjorden and Duvefjorden, northern Nordaustlandet, Svalbard. *Journal of Quaternary Science*, 32(3), 437-455. DOI: 10.1002/jqs.2938
- Fronval, T., & Jansen, E. (1996). Rapid changes in ocean circulation and heat flux in the Nordic seas during the last interglacial period. *Nature*, 383(6603), 806.
- Gebhardt, A. C., Geissler, W. H., Matthiessen, J., & Jokat, W. (2014). Changes in current patterns in the Fram Strait at the Pliocene/Pleistocene boundary. *Quaternary Science Reviews*, 92, 179-189. <http://dx.doi.org/10.1016/j.quascirev.2013.07.015>
- Geissler, W., Jokat, W., & Brekke, H. (2011). The Yermak Plateau in the Arctic Ocean in the light of reflection seismic data-implication for its tectonic and sedimentary evolution. *Geophysical Journal International*, 187(3), 1334-1362. doi: 10.1111/j.1365-246X.2011.05197.x
- Geissler, W. H., Gebhardt, A. C., Gross, F., Wollenburg, J., Jensen, L., Schmidt-Aursch, M. C., Krastel, S., Elger, J., & Osti, G. (2016). Arctic megaslide at presumed rest. *Scientific reports*, 6, 38529. DOI: 10.1038/srep38529
- Geissler, W. H., & Jokat, W. (2004). A geophysical study of the northern Svalbard continental margin. *Geophysical Journal International*, 158(1), 50-66. DOI: 10.1038/srep38529
- Geissler, W. H., Knies, J., Nielsen, T., Gaina, C., Matthiessen, J., Gebhardt, C., Damm, V., Forwick, M., Hjelstuen, B. O., & Hopper, J. R. (2014). The Opening of the Arctic-Atlantic Gateway: Tectonic, Oceanographic and Climatic Dynamics-an IODP Initiative. Paper presented at AGU Fall Meeting Abstracts, San Francisco, USA.
- Green, P., & Duddy, I. (2010). Synchronous exhumation events around the Arctic including examples from Barents Sea and Alaska North Slope. *Geological Society of London, Petroleum Geology Conference series*, 7, 633-644. DOI: 10.1144/0070633
- Haflidason, H., Sejrup, H. P., Nygård, A., Mienert, J., Bryn, P., Lien, R., Forsberg, C. F., Berg, K., & Masson, D. (2004). The Storegga Slide: architecture, geometry and slide development. *Marine Geology*, 213(1-4), 201-234. doi:10.1016/j.margeo.2004.10.007
- Hein, J. R., Konstantinova, N., Mikesell, M., Mizell, K., Fitzsimmons, J. N., Lam, P. J., Jensen, L. T., Xiang, Y., Gartman, A., & Cherkashov, G. (2017). Arctic Deep Water Ferromanganese- Oxide Deposits Reflect the Unique Characteristics of the Arctic Ocean. *Geochemistry, Geophysics, Geosystems*, 18(11), 3771-3800.
- Henriksen, E., Bjørnseth, H., Hals, T., Heide, T., Kiryukhina, T., Kløvjan, O., Larssen, G., Ryseth, A., Rønning, K., & Sollid, K. (2011). Uplift and erosion of the greater Barents Sea: impact on prospectivity and petroleum systems. *Geological Society of London, Memoirs*, 35(1), 271-281. DOI: 10.1144/M35.17
- Hernández-Molina, F., Llave, E., & Stow, D. (2008). Continental slope contourites. *Developments in Sedimentology*, 60, 379-408. DOI: 10.1016/S0070-4571(08)00219-7

- Hjelstuen, B. O., Eldholm, O., & Faleide, J. I. (2007). Recurrent Pleistocene mega-failures on the SW Barents Sea margin. *Earth and Planetary Science Letters*, 258(3), 605-618. doi:10.1016/j.epsl.2007.04.025
- Hjelstuen, B. O., Elverhøi, A., & Faleide, J. I. (1996). Cenozoic erosion and sediment yield in the drainage area of the Storfjorden Fan. *Global and Planetary Change*, 12(1), 95-117.
- Hogan, K., Dowdeswell, J., Noormets, R., Evans, J., Cofaigh, C. Ó., & Jakobsson, M. (2010). Submarine landforms and ice-sheet flow in the Kvitøya Trough, northwestern Barents Sea. *Quaternary Science Reviews*, 29(25), 3545-3562. doi:10.1016/j.quascirev.2010.08.015
- Hormes, A., Akçar, N., & Kubik, P. W. (2011). Cosmogenic radionuclide dating indicates ice-sheet configuration during MIS 2 on Nordaustlandet, Svalbard. *Boreas*, 40(4), 636-649. DOI 10.1111/j.1502-3885.2011.00215.x
- IHO International Hydrographic Organization (2002). S-23 Limits of Oceans and Seas Rep. Retrieved from https://www.iho.int/mtg_docs/com_wg/S-23WG/S-23WG_Misc/Draft_2002/Draft_2002.htm
- Jackson, H. R., Johnson, G. L., Sundvor, E., & Myhre, A. M. (1984). The Yermak Plateau: formed at a triple junction. *Journal of Geophysical Research: Solid Earth*, 89(B5), 3223-3232. <https://doi.org/10.1029/JB089iB05p03223>
- Jakobsson, M. (2002). Hypsometry and volume of the Arctic Ocean and its constituent seas. *Geochemistry, Geophysics, Geosystems*, 3(5), 1-18.
- Jakobsson, M., Andreassen, K., Bjarnadóttir, L. R., Dove, D., Dowdeswell, J. A., England, J. H., Funder, S., Hogan, K., Ingólfsson, Ó., & Jennings, A. (2014). Arctic Ocean glacial history. *Quaternary Science Reviews*, 92, 40-67. <http://dx.doi.org/10.1016/j.quascirev.2013.07.033>
- Jakobsson, M., Backman, J., Rudels, B., Nycander, J., Frank, M., Mayer, L., Jokat, W., Sangiorgi, F., O'Regan, M., & Brinkhuis, H. (2007). The early Miocene onset of a ventilated circulation regime in the Arctic Ocean. *Nature*, 447(7147), 986-990. doi:10.1038/nature05924
- Jansen, E., Fronval, T., Rack, F., & Channell, J. E. (2000). Pliocene- Pleistocene ice rafting history and cyclicity in the Nordic Seas during the last 3.5 Myr. *Paleoceanography*, 15(6), 709-721.
- Jokat, W. (2005). The sedimentary structure of the Lomonosov Ridge between 88 N and 80 N. *Geophysical Journal International*, 163(2), 698-726. doi: 10.1111/j.1365-246X.2005.02786.x
- Jokat, W., Geissler, W., & Voss, M. (2008). Basement structure of the north- western Yermak Plateau. *Geophysical Research Letters*, 35(5). doi:10.1029/2007GL032892
- Jokat, W., Lehmann, P., Damaske, D., & Nelson, J. B. (2016). Magnetic signature of North-East Greenland, the Morris Jesup Rise, the Yermak Plateau, the central Fram Strait: Constraints for the rift/drift history between Greenland and Svalbard since the Eocene. *Tectonophysics*, 691, 98-109. <http://dx.doi.org/10.1016/j.tecto.2015.12.002>
- Jokat, W., & Micksch, U. (2004). Sedimentary structure of the Nansen and Amundsen basins, Arctic Ocean. *Geophysical Research Letters*, 31(2). doi:10.1029/2003GL018352
- Karasik, A. (1968). Magnetic anomalies of the Gakkel Ridge and origin of the Eurasia Subbasin of the Arctic Ocean. *Geophys. Methods Prospect. Arctic*, 5, 8-19.
- King, E., Haflidason, H., Sejrup, H., & Løvlie, R. (1998). Glacigenic debris flows on the North Sea Trough Mouth Fan during ice stream maxima. *Marine Geology*, 152(1-3), 217-246.
- King, E. L., Sejrup, H. P., Haflidason, H., Elverhøi, A., & Aarseth, I. (1996). Quaternary seismic stratigraphy of the North Sea Fan: glacially-fed gravity flow aprons, hemipelagic sediments, and large submarine slides. *Marine Geology*, 130(3-4), 293-315.
- Kleiber, H., Knies, J., & Niessen, F. (2000). The Late Weichselian glaciation of the Franz Victoria Trough, northern Barents Sea: ice sheet extent and timing. *Marine Geology*, 168(1), 25-44.
- Kleiven, H. F., Jansen, E., Fronval, T., & Smith, T. (2002). Intensification of Northern Hemisphere glaciations in the circum Atlantic region (3.5–2.4 Ma)–ice-rafted detritus evidence. *Palaeogeography, Palaeoclimatology, Palaeoecology*, 184(3-4), 213-223.
- Knies, J., & Gaina, C. (2008). Middle Miocene ice sheet expansion in the Arctic: Views from the Barents Sea. *Geochemistry, Geophysics, Geosystems*, 9(2). doi:10.1029/2007GC001824
- Knies, J., Matthiessen, J., Vogt, C., Laberg, J. S., Hjelstuen, B. O., Smelror, M., Larsen, E., Andreassen, K., Eidvin, T., & Vorren, T. O. (2009). The Plio-Pleistocene glaciation of the Barents Sea–Svalbard region: a new model based on revised chronostratigraphy. *Quaternary Science Reviews*, 28(9), 812-829. doi:10.1016/j.quascirev.2008.12.002
- Knies, J., Mattingsdal, R., Fabian, K., Grøsfjeld, K., Baranwal, S., Husum, K., De Schepper, S., Vogt, C., Andersen, N., & Matthiessen, J. (2014). Effect of early Pliocene uplift on late Pliocene cooling in the Arctic–Atlantic gateway. *Earth and Planetary Science Letters*, 387, 132-144. <http://dx.doi.org/10.1016/j.epsl.2013.11.007>
- Kristoffersen, Y. (1990). On the tectonic evolution and paleoceanographic significance of the Fram Strait gateway, in *Geological history of the polar oceans: arctic versus antarctic*. edited, pp. 63-76, Springer,

- Kristoffersen, Y., Sorokin, M. Y., Jokat, W., & Svendsen, O. (2004). A submarine fan in the Amundsen Basin, Arctic Ocean. *Marine Geology*, 204(3-4), 317-324. [https://doi.org/10.1016/S0025-3227\(03\)00373-6](https://doi.org/10.1016/S0025-3227(03)00373-6)
- Kuvaas, B., & Kristoffersen, Y. (1991). The Crary Fan: a trough-mouth fan on the Weddell Sea continental margin, Antarctica. *Marine Geology*, 97(3-4), 345-362.
- Laberg, J., & Camerlenghi, A. (2008). The significance of contourites for submarine slope stability. *Developments in Sedimentology*, 60, 537-556. [https://doi.org/10.1016/S0070-4571\(08\)10025-5](https://doi.org/10.1016/S0070-4571(08)10025-5)
- Laberg, J., Eilertsen, R., & Vorren, T. (2009). The paleo-ice stream in Vestfjorden, north Norway, over the last 35 ky: Glacial erosion and sediment yield. *Geological Society of America Bulletin*, 121(3-4), 434-447.
- Laberg, J., & Vorren, T. (1995). Late Weichselian submarine debris flow deposits on the Bear Island Trough mouth fan. *Marine Geology*, 127(1), 45-72.
- Laberg, J., & Vorren, T. (1996). The Middle and Late Pleistocene evolution and the Bear Island Trough Mouth Fan, *Global and Planetary Change*, 12(1), 309-330.
- Laberg, J., Vorren, T., Dowdeswell, J., Kenyon, N., & Taylor, J. (2000). The Andøya Slide and the Andøya Canyon, north-eastern Norwegian-Greenland Sea. *Marine Geology*, 162(2-4), 259-275.
- Laberg, J., Vorren, T., & Knutsen, S.-M. (1999). The Lofoten contourite drift off Norway. *Marine Geology*, 159(1), 1-6.
- Laberg, J., Vorren, T., Mienert, J., Evans, D., Lindberg, B., Ottesen, D., Kenyon, N., & Henriksen, S. (2002). Late Quaternary palaeoenvironment and chronology in the Trænadjupet Slide area offshore Norway. *Marine Geology*, 188(1-2), 35-60.
- Laberg, J. S., Andreassen, K., Knies, J., Vorren, T. O., & Winsborrow, M. (2010). Late Pliocene-Pleistocene development of the Barents Sea ice sheet. *Geology*, 38(2), 107-110. doi: 10.1130/G30193.1
- Laberg, J. S., Andreassen, K., & Vorren, T. O. (2012). Late Cenozoic erosion of the high-latitude southwestern Barents Sea shelf revisited. *Geological Society of America Bulletin*, 124(1-2), 77-88. doi: 10.1130/B30340.1
- Laberg, J. S., Dahlgren, T., Vorren, T. O., Haflidason, H., & Bryn, P. (2001). Seismic analyses of Cenozoic contourite drift development in the Northern Norwegian Sea. *Marine Geophysical Research*, 22(5), 401-416.
- Laberg, J. S., Rydningen, T. A., Forwick, M., & Husum, K. (2018). Depositional processes on the distal Scoresby Trough Mouth Fan (ODP Site 987): Implications for the Pleistocene evolution of the Scoresby Sund Sector of the Greenland Ice Sheet. *Marine Geology*. <https://doi.org/10.1016/j.margeo.2017.11.018>
- Laberg, J. S., Stoker, M. S., Dahlgren, K. T., de Haas, H., Haflidason, H., Hjelstuen, B. O., Nielsen, T., Shannon, P. M., Vorren, T. O., & van Weering, T. C. (2005). Cenozoic alongslope processes and sedimentation on the NW European Atlantic margin. *Marine and Petroleum Geology*, 22(9), 1069-1088. doi:10.1016/j.marpetgeo.2005.01.008
- Lambeck, K. (1995). Constraints on the Late Weichselian ice sheet over the Barents Sea from observations of raised shorelines. *Quaternary Science Reviews*, 14(1), 1-16.
- Lambeck, K. (1996). Limits on the areal extent of the Barents Sea ice sheet in Late Weichselian time. *Global and Planetary Change*, 12(1-4), 41-51.
- Landvik, J. Y., Bondevik, S., Elverhøi, A., Fjeldskaar, W., Mangerud, J., Salvigsen, O., Siegert, M. J., Svendsen, J.-I., & Vorren, T. O. (1998). The last glacial maximum of Svalbard and the Barents Sea area: ice sheet extent and configuration. *Quaternary Science Reviews*, 17(1-3), 43-75.
- Larsen, H., Saunders, A., Clift, P., Beget, J., Wei, W., & Spezzaferrri, S. (1994). Seven million years of glaciation in Greenland. *Science*, 264(5161), 952-955.
- Lasabuda, A. (2018). Cenozoic tectonosedimentary development and erosion estimates for the Barents Sea continental margin, Norwegian Arctic. (Doctoral dissertation). Retrieved from Munin. (<http://hdl.handle.net/10037/12800>). Tromsø: UiT - The Arctic University of Norway
- Lasabuda, A., Laberg, J. S., Knutsen, S.-M., & Høgseth, G. (2018a). Early to middle Cenozoic paleoenvironment and erosion estimates of the southwestern Barents Sea: Insights from a regional mass-balance approach. *Marine and Petroleum Geology*, 96, 501-521. <https://doi.org/10.1016/j.marpetgeo.2018.05.039>
- Lasabuda, A., Laberg, J. S., Knutsen, S.-M., & Safronova, P. A. (2018b). Cenozoic tectonostratigraphy and pre-glacial erosion: A mass-balance study of the northwestern Barents Sea margin, Norwegian Arctic. *Journal of Geodynamics*. <https://doi.org/10.1016/j.jog.2018.03.004>
- Levitani, M. (2015). Sedimentation rates in the Arctic Ocean during the last five marine isotope stages. *Oceanology*, 55(3), 425-433.
- Mangerud, J., Jansen, E., & Landvik, J. Y. (1996). Late Cenozoic history of the Scandinavian and Barents Sea ice sheets. *Global and Planetary Change*, 12(1-4), 11-26.
- Manley, T., Bourke, R., & Hunkins, K. (1992). Near-surface circulation over the Yermak Plateau in northern Fram Strait. *Journal of Marine Systems*, 3(1-2), 107-125.

- Matthiessen, J., Knies, J., Vogt, C., & Stein, R. (2009). Pliocene palaeoceanography of the Arctic Ocean and subarctic seas. *Philosophical Transactions of the Royal Society of London A: Mathematical, Physical and Engineering Sciences*, 367(1886), 21-48. doi:10.1098/rsta.2008.0203
- Mattingsdal, R., Knies, J., Andreassen, K., Fabian, K., Husum, K., Grøsfjeld, K., & De Schepper, S. (2014). A new 6 Myr stratigraphic framework for the Atlantic–Arctic Gateway. *Quaternary Science Reviews*, 92, 170-178. <http://dx.doi.org/10.1016/j.quascirev.2013.08.022>
- Minakov, A., Faleide, J. I., Glebovsky, V. Y., & Mjelde, R. (2012). Structure and evolution of the northern Barents-Kara Sea continental margin from integrated analysis of potential fields, bathymetry and sparse seismic data. *Geophysical Journal International*, 188(1), 79-102. doi: 10.1111/j.1365-246X.2011.05258.x
- Minakov, A., Podladchikov, Y. Y., Faleide, J., & Huisman, R. (2013). Rifting assisted by shear heating and formation of the Lomonosov Ridge. *Earth and Planetary Science Letters*, 373, 31-40.
- Mitchum Jr, R., Vail, P., & Sangree, J. (1977). Seismic stratigraphy and global changes of sea level: Part 6. Stratigraphic interpretation of seismic reflection patterns in depositional sequences: Section 2. Application of seismic reflection configuration to stratigraphic interpretation.
- Moran, K., Backman, J., Brinkhuis, H., Clemens, S. C., Cronin, T., Dickens, G. R., Eynaud, F., Gattacceca, J., Jakobsson, M., & Jordan, R. W. (2006). The cenozoic palaeoenvironment of the arctic ocean. *Nature*, 441(7093), 601-605. doi:10.1038/nature04800
- Mosher, D. C., Campbell, D., Gardner, J., Piper, D., Chaytor, J., & Rebesco, M. (2017). The role of deep-water sedimentary processes in shaping a continental margin: The Northwest Atlantic. *Marine Geology*. <http://dx.doi.org/10.1016/j.margeo.2017.08.018>
- Mudsee, M., & Raymo, M. E. (2005). Slow dynamics of the Northern Hemisphere glaciation. *Paleoceanography*, 20(4). doi:10.1029/2005PA001153
- Nielsen, T., De Santis, L., Dahlgren, K., Kuijpers, A., Laberg, J., Nygård, A., Praeg, D., & Stoker, M. (2005). A comparison of the NW European glaciated margin with other glaciated margins. *Marine and Petroleum Geology*, 22(9-10), 1149-1183. doi:10.1016/j.marpetgeo.2004.12.007
- Nyland, B., Jensen, L., Skagen, J., Skarpnes, O., & Vorren, T. (1992). Tertiary uplift and erosion in the Barents Sea: magnitude, timing and consequences. *Tectonic Modelling and Its Implication to Petroleum Geology*; Larsen, RM, Brekke, H., Larsen, BT, Talleras, E., Eds, 153-162.
- Osti, G., Franek, P., Forwick, M., & Laberg, J. S. (2017). Controlling factors for slope instability in a seismically active region: The NW-Svalbard continental margin. *Marine Geology*, 390, 131-146.
- Ottesen, D., Dowdeswell, J., & Rise, L. (2005). Submarine landforms and the reconstruction of fast-flowing ice streams within a large Quaternary ice sheet: The 2500-km-long Norwegian-Svalbard margin (57–80 N). *Geological Society of America Bulletin*, 117(7-8), 1033-1050. doi: 10.1130/B25577.1
- Patton, H., Andreassen, K., Bjarnadóttir, L. R., Dowdeswell, J. A., Winsborrow, M., Noormets, R., Polyak, L., Auriac, A., & Hubbard, A. (2015). Geophysical constraints on the dynamics and retreat of the Barents Sea ice sheet as a paleobenchmark for models of marine ice sheet deglaciation. *Reviews of Geophysics*, 53(4), 1051-1098. doi:10.1002/2015RG000495
- Pérez, L. F., & Nielsen, T. (2017). Asynchronous ice-sheet development along the central East Greenland margin: a GLANAM project contribution. *Geological Survey of Denmark and Greenland Bulletin*(38), 61-64.
- Posamentier, H. W., & Kolla, V. (2003). Seismic geomorphology and stratigraphy of depositional elements in deep-water settings. *Journal of Sedimentary Research*, 73(3), 367-388.
- Rasmussen, E., & Fjeldskaar, W. (1996). Quantification of the Pliocene-Pleistocene erosion of the Barents Sea from present-day bathymetry. *Global and Planetary Change*, 12(1), 119-133.
- Rebesco, M., & Camerlenghi, A. (2008). Late Pliocene margin development and mega debris flow deposits on the Antarctic continental margins: Evidence of the onset of the modern Antarctic Ice Sheet? *Palaeogeography, Palaeoclimatology, Palaeoecology*, 260(1-2), 149-167.
- Rebesco, M., Hernández-Molina, F. J., Van Rooij, D., & Wählin, A. (2014). Contourites and associated sediments controlled by deep-water circulation processes: state-of-the-art and future considerations. *Marine Geology*, 352, 111-154. <http://dx.doi.org/10.1016/j.margeo.2014.03.011>
- Riis, F., & Fjeldskaar, W. (1992). On the magnitude of the Late Tertiary and Quaternary erosion and its significance for the uplift of Scandinavia and the Barents Sea, in *Structural and tectonic modelling and its application to petroleum geology*. edited by R. M. Larsen, H. Brekke, B. T. Larsen & E. Taleraas, pp. 163-185, Norw. Petrol. Soc.,
- Rydningen, T. A., Laberg, J. S., & Kolstad, V. (2016). Late Cenozoic evolution of high-gradient trough mouth fans and canyons on the glaciated continental margin offshore Troms, northern Norway—Paleoclimatic implications and sediment yield. *Geological Society of America Bulletin*, 128(3-4), 576-596. doi: 10.1130/B31302.1

- Rydningen, T. A., Vorren, T. O., Laberg, J. S., & Kolstad, V. (2013). The marine-based NW Fennoscandian ice sheet: glacial and deglacial dynamics as reconstructed from submarine landforms. *Quaternary Science Reviews*, 68, 126-141. <http://dx.doi.org/10.1016/j.quascirev.2013.02.013>
- Safronova, P., Laberg, J., Andreassen, K., Shlykova, V., Vorren, T., & Chernikov, S. (2015). Late Pliocene–early Pleistocene deep-sea basin sedimentation at high-latitudes: mega-scale submarine slides of the north-western Barents Sea margin prior to the shelf-edge glaciations. *Basin Research*, 1-19. doi: 10.1111/bre.12161
- Solheim, A., Faleide, J. I., Andersen, E. S., Elverhøi, A., Forsberg, C. F., Vanneste, K., Uenzelmann-Neben, G., & Channell, J. E. (1998). Late Cenozoic seismic stratigraphy and glacial geological development of the East Greenland and Svalbard–Barents Sea continental margins. *Quaternary Science Reviews*, 17(1-3), 155-184.
- Srivastava, S. (1985). Evolution of the Eurasian Basin and its implications to the motion of Greenland along Nares Strait. *Tectonophysics*, 114(1-4), 29-53.
- Srivastava, S., & Tapscott, C. (1986). Plate kinematics of the North Atlantic. *The Geology of North America*, 1000, 379-404.
- St John, K. (2008). Cenozoic ice-rafting history of the central Arctic Ocean: Terrigenous sands on the Lomonosov Ridge. *Paleoceanography*, 23(1). doi:10.1029/2007PA001483
- Stoker, M. S., Praeg, D., Hjelstuen, B. O., Laberg, J. S., Nielsen, T., & Shannon, P. M. (2005). Neogene stratigraphy and the sedimentary and oceanographic development of the NW European Atlantic margin. *Marine and Petroleum Geology*, 22(9-10), 977-1005. doi:10.1016/j.marpetgeo.2004.11.007
- Stow, D., Hunter, S., Wilkinson, D., & Hernández-Molina, F. (2008). The nature of contourite deposition. *Developments in Sedimentology*, 60, 143-156.
- Stow, D., & Lovell, J. (1979). Contourites: their recognition in modern and ancient sediments. *Earth-Science Reviews*, 14(3), 251-291.
- Svendsen, J. I., Alexanderson, H., Astakhov, V. I., Demidov, I., Dowdeswell, J. A., Funder, S., Gataullin, V., Henriksen, M., Hjort, C., & Houmark-Nielsen, M. (2004). Late Quaternary ice sheet history of northern Eurasia. *Quaternary Science Reviews*, 23(11), 1229-1271. doi:10.1016/j.quascirev.2003.12.008
- Svindland, K., & Vorren, T. (2002). Late Cenozoic sedimentary environments in the Amundsen Basin, Arctic ocean. *Marine Geology*, 186(3-4), 541-555.
- Talwani, M., & Eldholm, O. (1977). Evolution of the Norwegian-Greenland sea. *Geological Society of America Bulletin*, 88(7), 969-999.
- Vanneste, M., Mienert, J., & Bünz, S. (2006). The Hinlopen Slide: a giant, submarine slope failure on the northern Svalbard margin, Arctic Ocean. *Earth and Planetary Science Letters*, 245(1), 373-388. doi:10.1016/j.epsl.2006.02.045
- Vogt, P. R., & Avery, O. E. (1974). Tectonic history of the Arctic basins: Partial solutions and unsolved mysteries, in *Marine geology and oceanography of the Arctic Seas*. edited, pp. 83-117, Springer,
- Vorren, T. O., & Laberg, J. S. (1997). Trough mouth fans—palaeoclimate and ice-sheet monitors. *Quaternary Science Reviews*, 16(8), 865-881.
- Vorren, T. O., Laberg, J. S., Blaume, F., Dowdeswell, J. A., Kenyon, N. H., Mienert, J., Rumohr, J., & Werner, F. (1998). The Norwegian–Greenland Sea continental margins: morphology and late Quaternary sedimentary processes and environment. *Quaternary Science Reviews*, 17(1-3), 273-302.
- Vorren, T. O., Landvik, J. Y., Andreassen, K., & Laberg, J. S. (2011). Glacial history of the Barents Sea region. *Quaternary Glaciations—Extent and Chronology—A Closer Look*, *Dev. in Quat. Sci.*, 361-372. doi: 10.1016/B978-0-444-53447-7.00027-1
- Vorren, T. O., Richardsen, G., Knutsen, S.-M., & Henriksen, E. (1991). Cenozoic erosion and sedimentation in the western Barents Sea. *Marine and Petroleum Geology*, 8(3), 317-340.
- Våagnes, E. (1996). Cenozoic deposition in the Nansen Basin, a first-order estimate based on present-day bathymetry. *Global and Planetary Change*, 12(1-4), 149-157.
- Winkelmann, D., Geissler, W., Schneider, J., & Stein, R. (2008). Dynamics and timing of the Hinlopen/Yermak Megaslide north of Spitsbergen, Arctic Ocean. *Marine Geology*, 250(1), 34-50. doi:10.1016/j.margeo.2007.11.013

Table 1
Measurements for the Depositional Area

Unit	Age range [Ma]	Age interval [Ma]	Velocity average [km/s]	Sediment volume [10^3 km^3]	Depositional area [10^3 km^2]	Avg. sedimentation rates [m/Kyr]
NB-3C	0 – 0.7	0.7	1.7	0.7	8	0.12
NB-3B	0.7 – 1.5	0.8	1.9	17	28	0.77
NB-3A	1.5 – 2.7	1.2	1.9	11	44	0.2
Plio–Pleistocene	0 – 2.7	2.7	1.9	29	44	0.24

Note. Sediment volumes, depositional areas, and sedimentation rates for the glacial strata. Here, the NB-3A sediment volume has not been reduced by 10% to account for contouritic deposits. The geologic timescale is according to Cohen et al. (2016).

Accepted Article

Table 2*Measurements for the Source Area*

Unit	Age range [Ma]	Volume of the source area [10 ³ km ³]		Source area [10 ³ km ²]		Sediment discharge [10 ⁶ t/yr] with sediment density 2.2 g/cm ³		Sediment yield [t/km ² /yr]		Avg. net erosion [m]		Avg. erosion rates [m/Kyr]	
		Min,	Max,	Min	Max	Min	Max	Min	Max	Min	Max	Min	Max
		with 20% bedrock composition correction	with 10% bedrock composition correction										
NB-3C	0–0.7	0.5	0.6	32	63	1.6	1.8	29	51	10	20	0.01	0.02
NB-3B	0.7–1.5	13	15	32	63	36	40	640	1120	230	400	0.29	0.51
NB-3A	1.5–2.7	7	8	32	49	13	15	310	420	170	230	0.14	0.19
Plio–Pleistocene	0–2.7	21	24	32	63	17	20	310	540	410	650	0.15	0.24

Note. Volume of the source area, source area, sediment discharge, sediment yield, average net erosion, and average erosion rates. The NB-3A sediment volume has been reduced by 10% correction due to deposition of contourites and another 5% due to compaction correction before applying the bedrock composition correction.

Table 3*Comparison of Our Results to Other Formerly Glaciated Margins*

Areas	Sedimentation rates [m/Kyr]	Source area [10^3 km ²]	Bedrock types in the source area	Volume of the source area [10^3 km ³]	Erosion [m]	Erosion Rates [m/Kyr]
Northeastern Svalbard (This study)	0.24	32 – 63	Crystalline + sedimentary rocks	21 – 24	410 – 650	0.15 – 0.24
Northwestern Barents Sea – Storffjorden Fan ^a	0.7	116	Sedimentary rocks	69	1700	0.63
Southwestern Barents Sea – Bjørnøya Fan ^b	0.16 – 0.64	576	Sedimentary rocks	395 – 464	1000 – 1100	0.38 – 0.41
Troms margin ^c	0.15 – 0.22	14 – 43	Crystalline rocks	2 – 2.2	50 – 140	0.02 – 0.05
Mid-Norway – NAUST Fm ^d	0.24	160	Crystalline rocks	83.7	524	0.19
Western Svalbard – Isfjorden Fan ^e	-	0.73	Crystalline + sedimentary rocks	0.32	-	0.2

^aHjelstuen et al. (1996). ^bLaberg et al. (2012). ^cRydningen et al. (2016). ^dDowdeswell et al. (2010b). ^eElverhøi, et al. (1998).

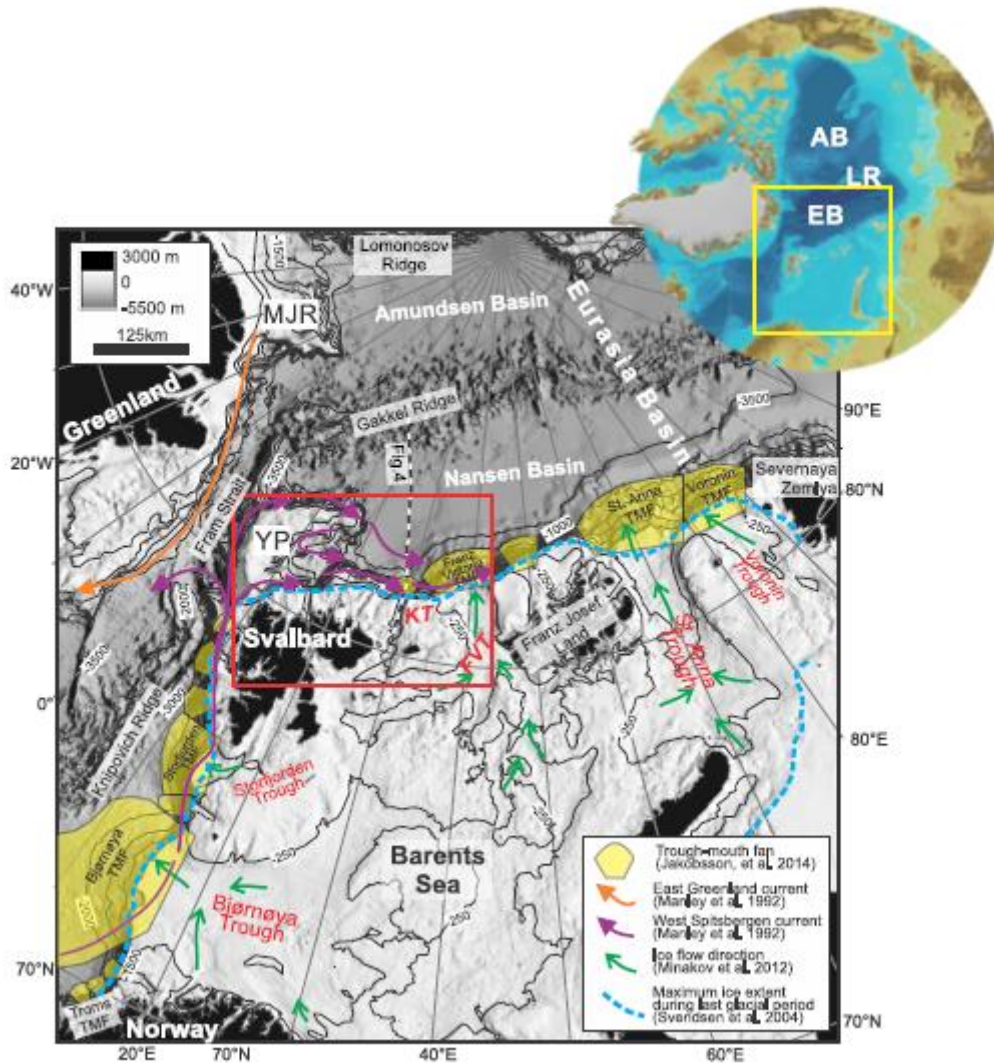


Figure 1. Regional geological setting of the Barents Sea shelf and the surroundings. The location of the study area is shown as red and yellow squares (inset figure). Bathymetry map is from International Bathymetry Chart of the Arctic Ocean (IBCAO) dataset v. 3.0 (Jakobsson et al., 2012) with WGS84 Polar Stereographic Projection. The location of Figure 4 is indicated by a black dashed line. AB=Amerasia Basin; EB=Eurasia Basin; LR=Lomonosov Ridge; FVT= Franz Victoria Trough; KT= Kvitøya Trough; MJR= Morris Jesup Rise; YP= Yermak Plateau.

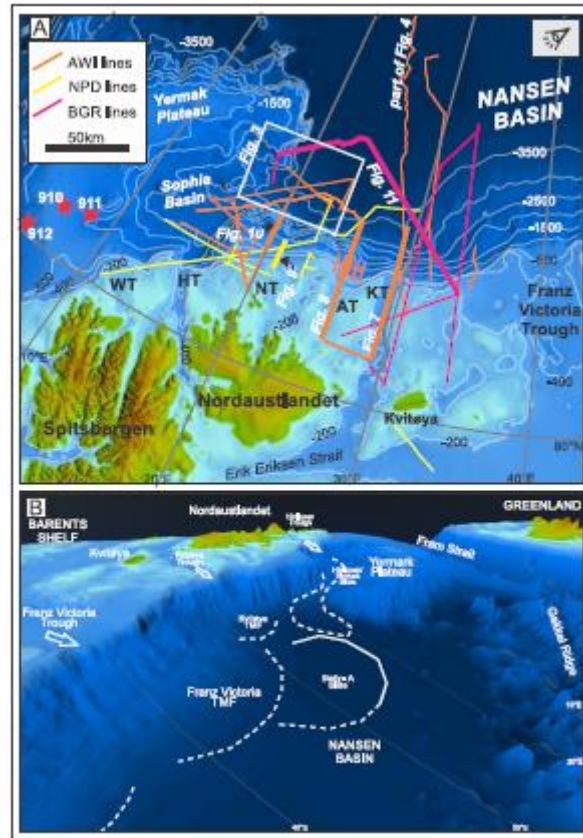


Figure 2. A) Seismic data distribution used in this study. Bathymetry map is taken from IBCAO dataset v. 3.0 (Jakobsson et al., 2012) with WGS84 Polar Stereographic Projection. Existing Ocean Drilling Program (ODP) sites are marked by stars. The location of Figures 7 – 11 are indicated as bold lines. The location of Figure 3 is shown as white rectangles. B) 3D visualization of the study area. Viewpoint is indicated at Figure 2A. Note the convex-outward shape in front of Franz Victoria Trough suggest a major trough-mouth fan development. Extent of Body A is uncertain to the east due to limited data coverage. WT=Woodfjorden Trough; HT=Hinlopen Trough; NT=Nordenskjold Trough (Cherkis et al., 1999); AT=Albertini Trough; KT=Kvitøya Trough

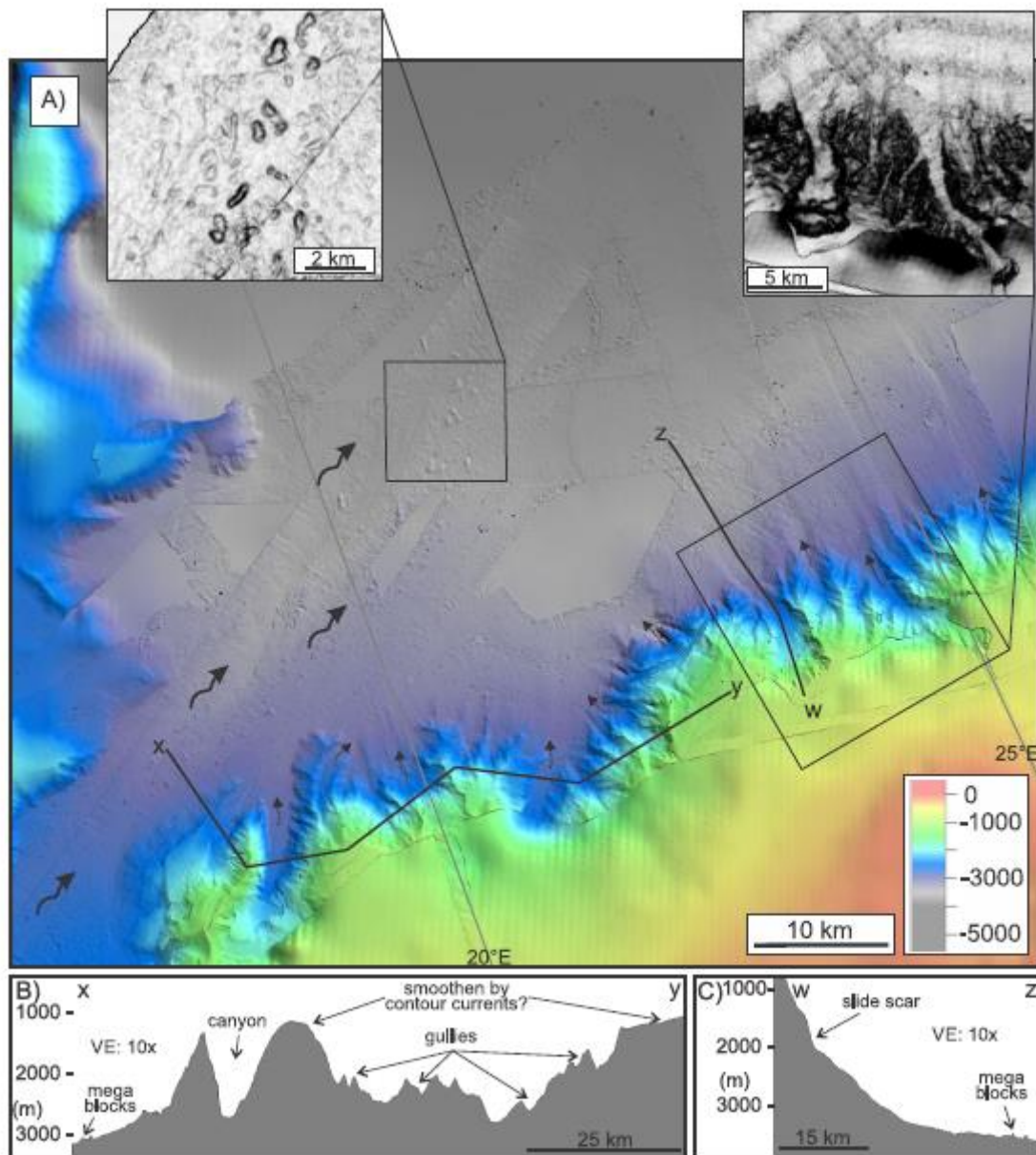


Figure 3. A) Seafloor bathymetry at the lower slope of the Nordenskjold Trough. In the Nansen Basin, a number of megablocks are observed interpreted as a result of Hinlopen/Yermak megaslide (Vanneste et al., 2006; Winkelmann et al., 2008). B) Seafloor profile along the lower slope morphology showing a number of canyons and gullies. C) Seafloor profile example crossing one of the major canyons showing a slide scar. For location, see Figure 2A.

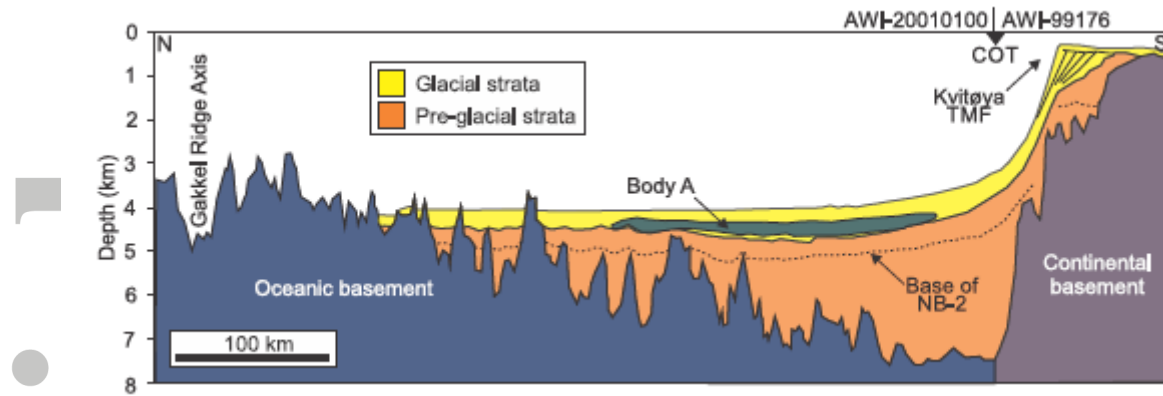


Figure 4. Geoseismic illustrating the general stratigraphy of the northeastern Svalbard / northern Barents Sea continental margin (modified after Jokat and Micksch, 2004). The profile represents subdivision of glacial and non/less-influenced glacial strata that will be used for sediment budgeting. The deposits from a large submarine slide, Body A, is shown. COT=continent-oceanic crust transition. Seismic location at Figure 1.

Accepted Article

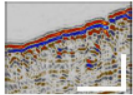
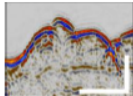
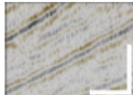
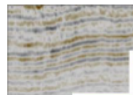
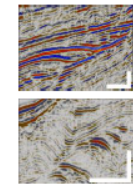
Seismic Facies (SF)	Description	Interpretation	Figure example
SF1a: Chaotic	Medium to high amplitude reflections, irregular top and base, internally chaotic but in some areas show imbricated pattern	Glacigenic/non-glacigenic debrites, slumps, slides, products of mass-wasting events. Together, SF1a and SF1b are termed mass-transport deposit (MTD). SF1a has probably coarser materials, meanwhile SF1b is mud-dominated deposit (see Posamentier & Kolla, 2003).	
SF1b: Semi-transparent	Low amplitude reflections, discontinuous, irregular top and base, internally structureless		
SF2: Tangential/oblique parallel	Low to medium amplitude reflections, continuous, stacked of angular packages, often truncated to the upper layer	Prograding glacigenic sedimentary wedges or widely known as glacial-sedimentary prism or trough-mouth fan (TMF). TMFs generally consist of variable lithologies representing glacigenic debris flow processes (e.g. Laberg & Vorren, 1995).	
SF3: Parallel to sub-parallel	Low to high amplitude reflections, continuous to semi-continuous, commonly conformable top and base	Depending of the location and the strata, this facies can be interpreted as the following: <ol style="list-style-type: none"> 1. Hemipelagic or glacimarine sediments. Glacimarine sediments formed as a result of slow-settling background sedimentation from iceberg (e.g. King et al., 1996). 2. Turbiditic sheets/fans of sand-shale interlayers 3. Sheeted drifts deposited by contour currents 	
SF4: Contorted	Low to high amplitude and discontinuous reflections at the axial part, typical V- or U-shaped morphology flanked by low to medium amplitude and relatively continuous reflections package	This facies is interpreted as sediment waves or contourite drifts, produced by contour currents as a result of ocean circulation. This package has typically a mud-rich lithology (see Rebesco et al., 2014).	

Figure 5. Seismic facies classification for the study area. The vertical and horizontal white bars represent 100 ms and 1 km, respectively.

Accepted

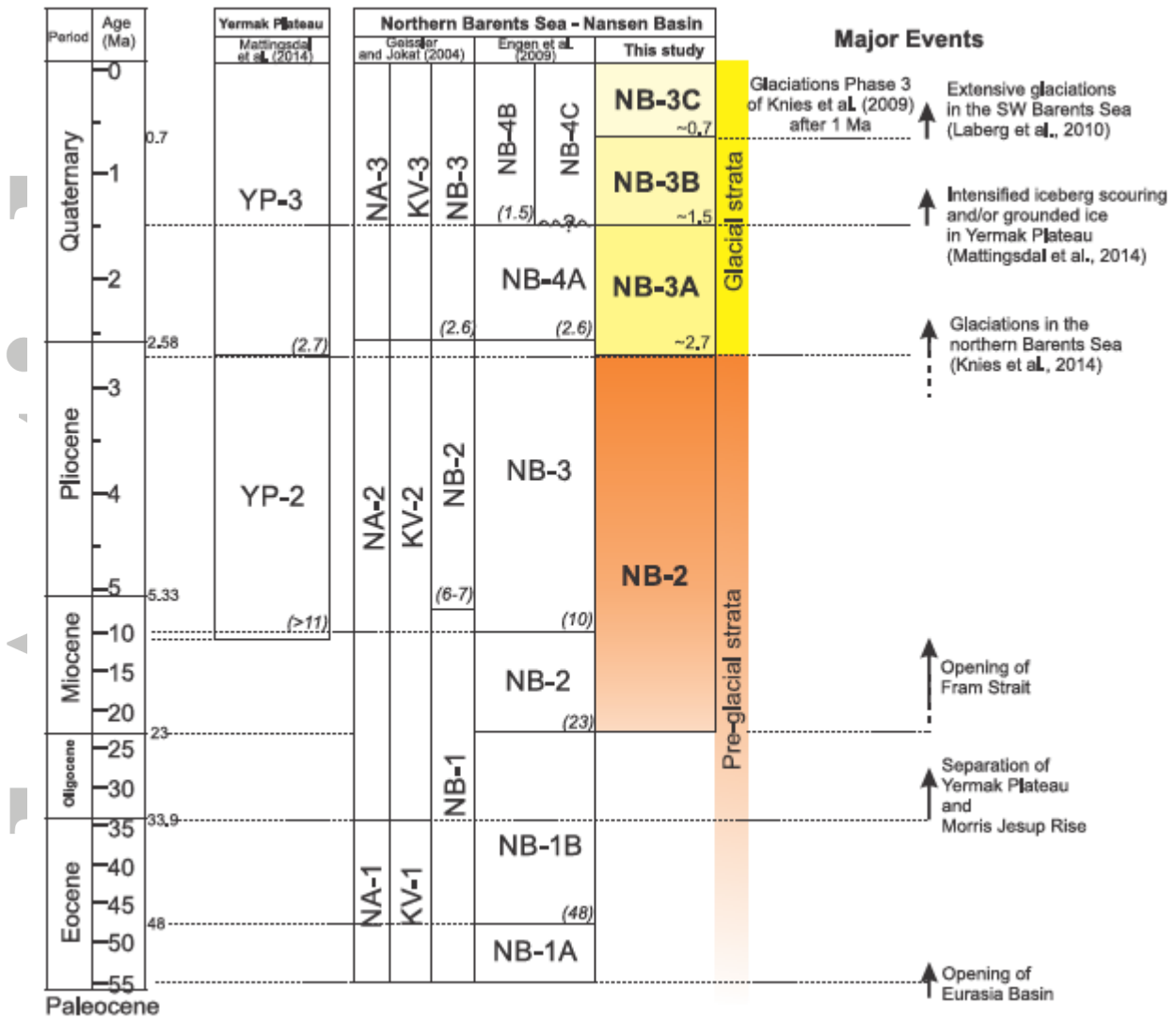


Figure 6. Chronology of the strata focused in this study (modified from Engen et al., 2009). The base of unit NB-3A (~2.7 Ma) is from Knies et al. (2014) and Mattingsdal et al. (2014). The base of unit NB-3B (~1.5 Ma) is from Mattingsdal et al. (2014). The base of unit NB-3C is from the inferred age model of Laberg et al. (2010) assuming that the base unit NB-3C in this study correlates to the base of unit GIII. The geologic timescale is according to Cohen et al. (2016).

Acce

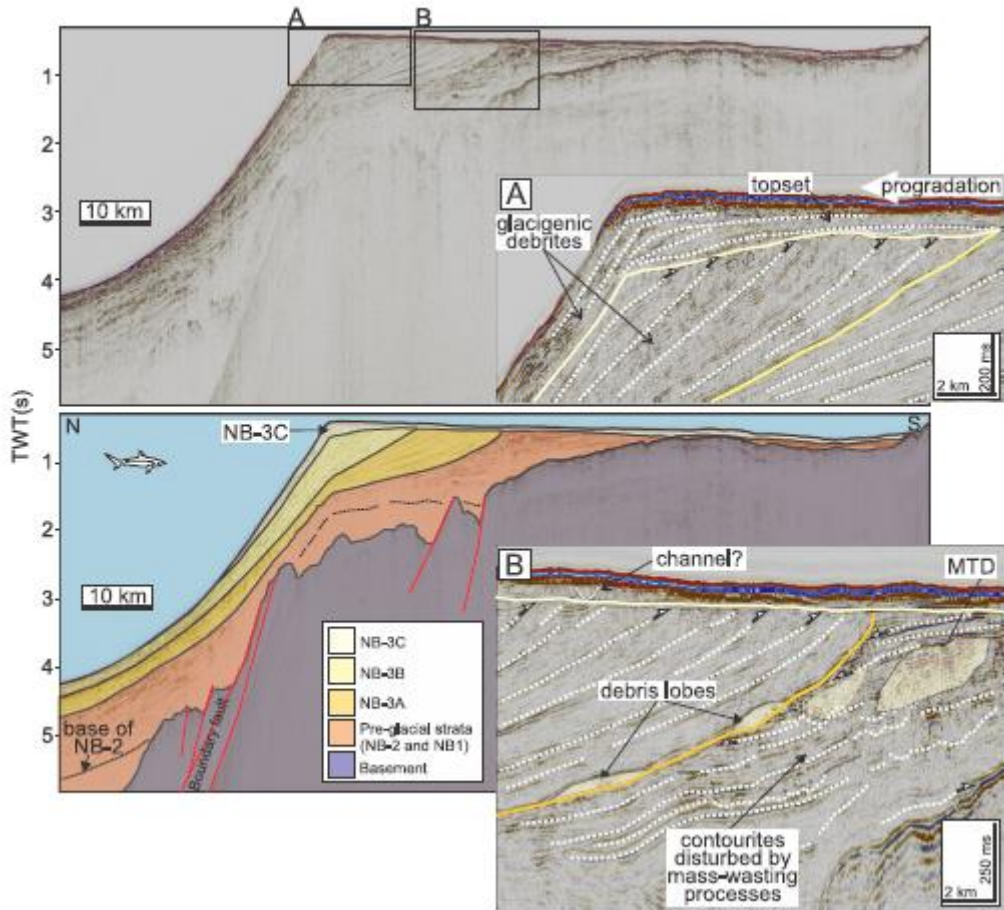


Figure 7. Seismic profile AWI-99176 (modified from Geissler & Jokat, 2004) illustrating the subdivision of Kvitøya TMF. A) Notable truncation of NB-3B can be seen at the base of NB-3C. NB-3C shows a lower angle progradation consisting of glacigenic debrites. NB-3C is regarded as the topset part of the TMF. B) Debris lobes at the base of NB-3A suggest a sign for an early phase of intensified glaciations. NB-2 reflections are truncated to the base NB-3A. For location, see Figure 2A.

Acce

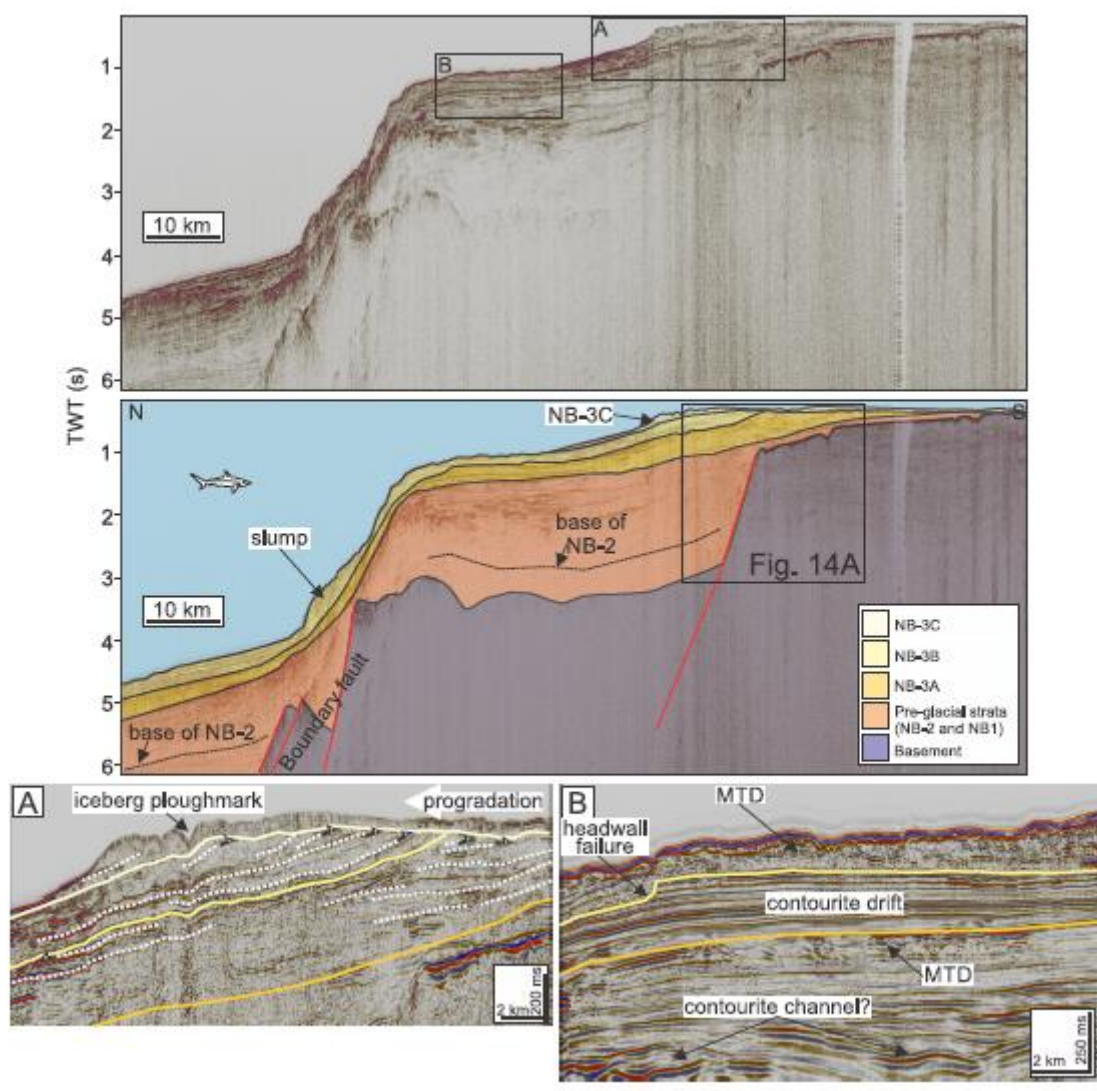


Figure 8. Seismic profile AWI-99170 (modified from Geissler & Jokat, 2004) showing sedimentary style in the Albertini Trough. A glacial-sedimentary prism appears to be less developed here compare to the Kvitøya Trough. A) Sediment progradations and development NB-3C suggest an episodic ice sheet advance in this trough. B) NB-3A shows a development of sheeted drift overlain by MTDs of NB-3B. For location, see Figure 2A.

Acce

▲
 ●
 ▲
 ▲

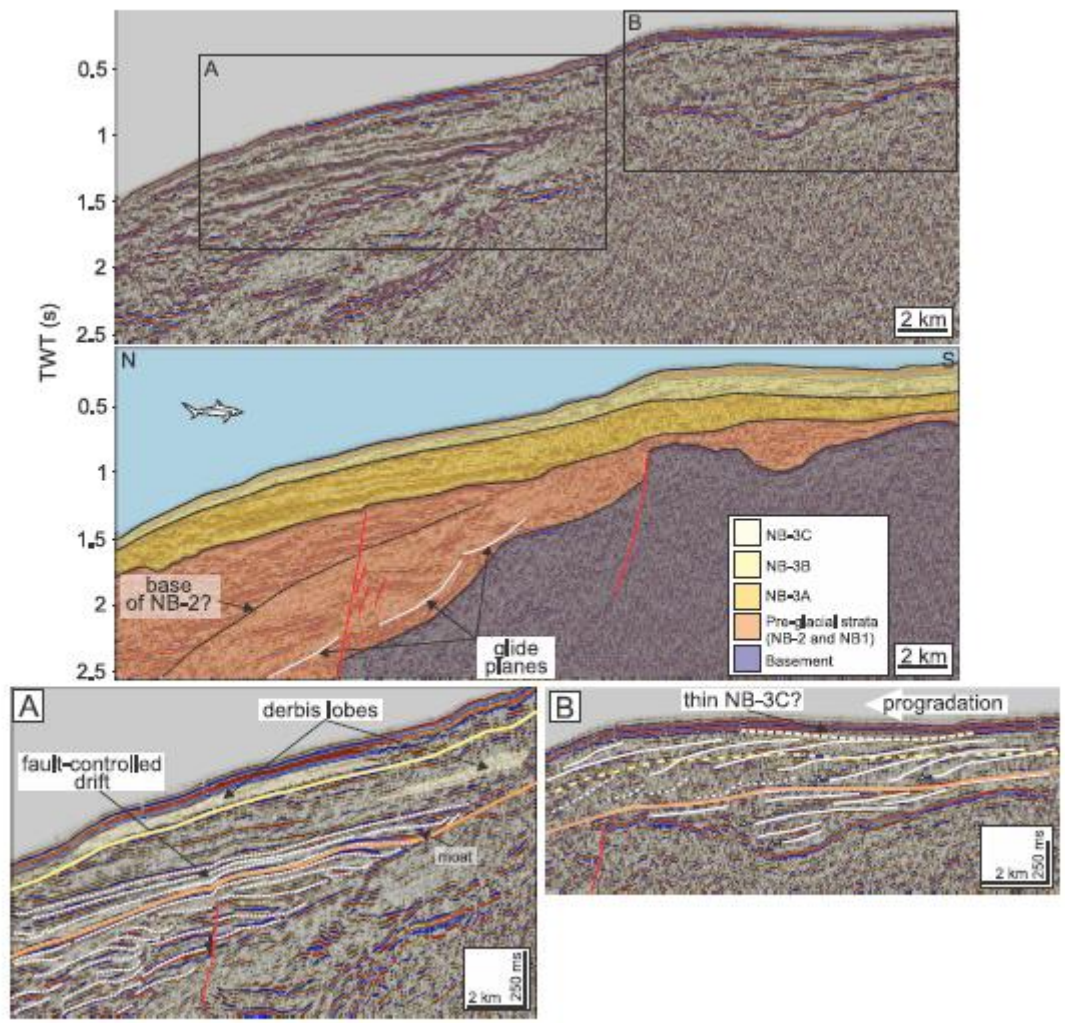


Figure 9. Seismic profile HAP0384 illustrating sedimentary development in Nordenskjold Trough. A) Upper slope is dominated by debris lobes in NB-3A and NB-3B. Meanwhile, pre-glacial strata shows a pronounced contourites development. B) Sedimentary style for glacial strata is observed as low-angle progradation and chaotic packages interpreted as MTDs. This area marks the western limits of NB-3C. For location, see Figure 2A.

Accepted

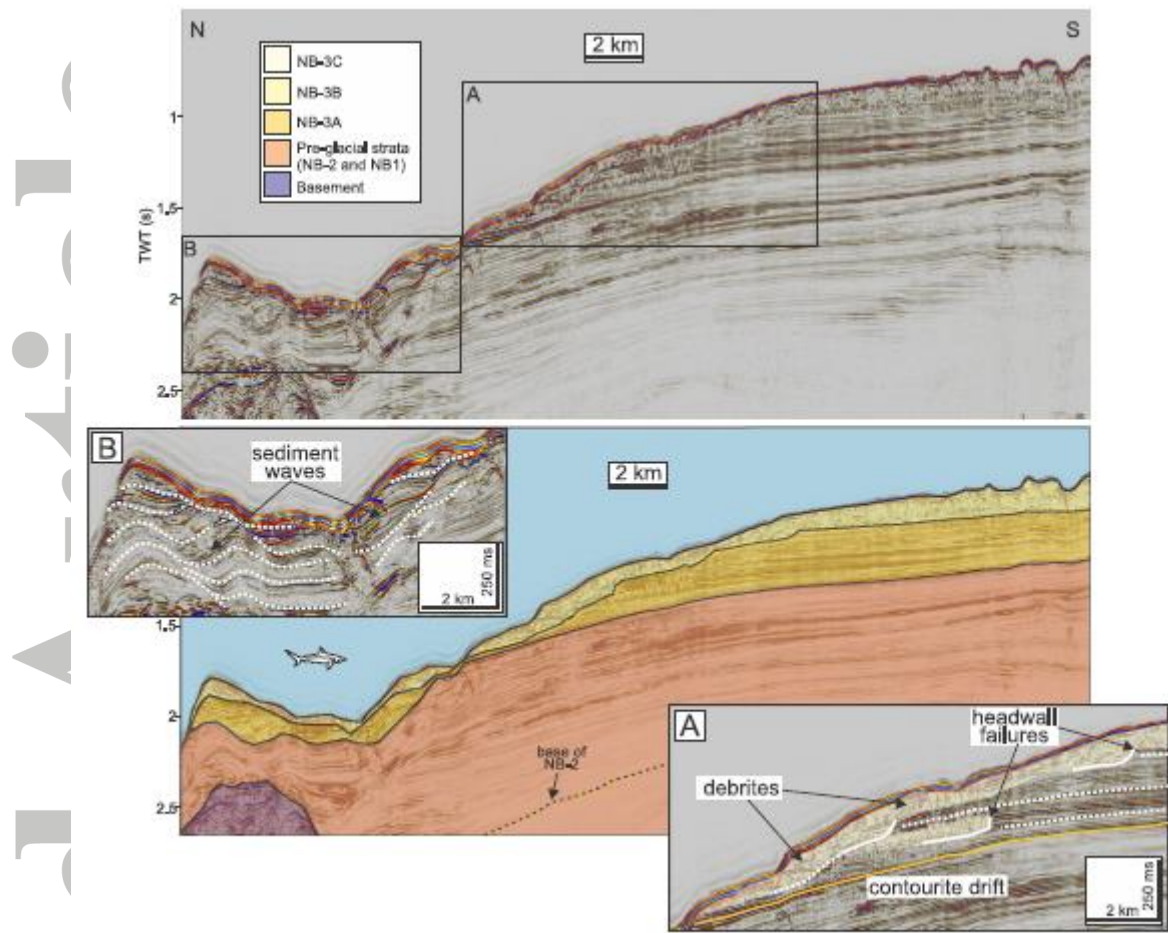


Figure 10. Seismic profile AWI-99130 west of Nordenskjold Trough showing a domination of contourites and sediment waves at NB-3A and older. A) NB-3A shows indication of headwall failures. B) NB-3A and NB-3B show sediment waves. For location, see Figure 2A.

Accepted Article

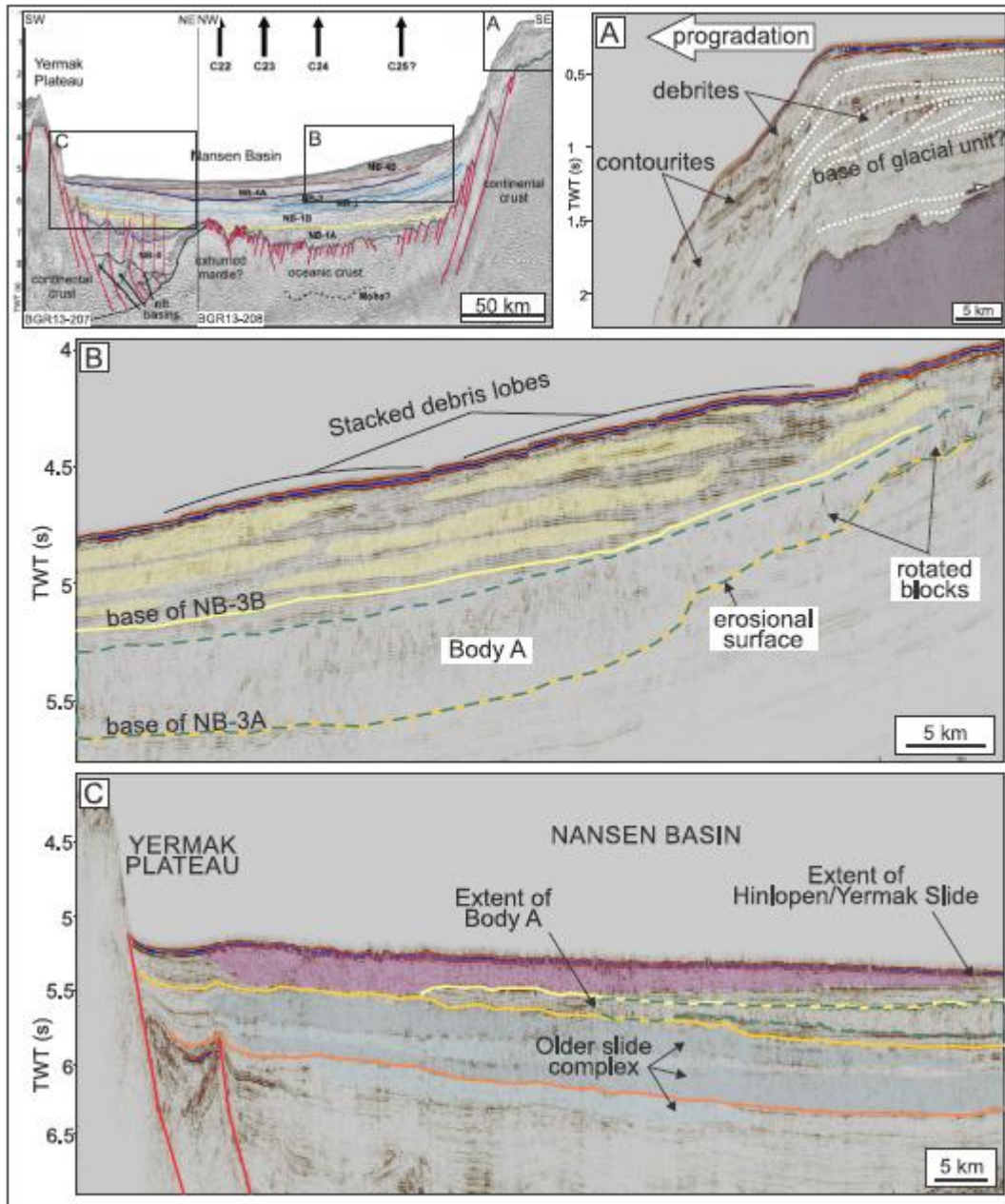


Figure 11. Seismic profile BGR13-207 and BGR13-208 (figure originally appeared in *Frontiers in Earth Science*, doi: 10.3389/feart.2016.00091, Berglar et al., 2016 with nomenclature following Engen et al., 2009). A) Sediment progradation is interpreted as part of Franz Victoria TMF. B) Stacked debris lobes suggest a domination of mass-wasting processes. C) The extent of Body A and Hinlopen/Yermak Slide (Vanneste et al., 2006, Winkelmann et al., 2008) can be mapped. For location, see Figure 2A.

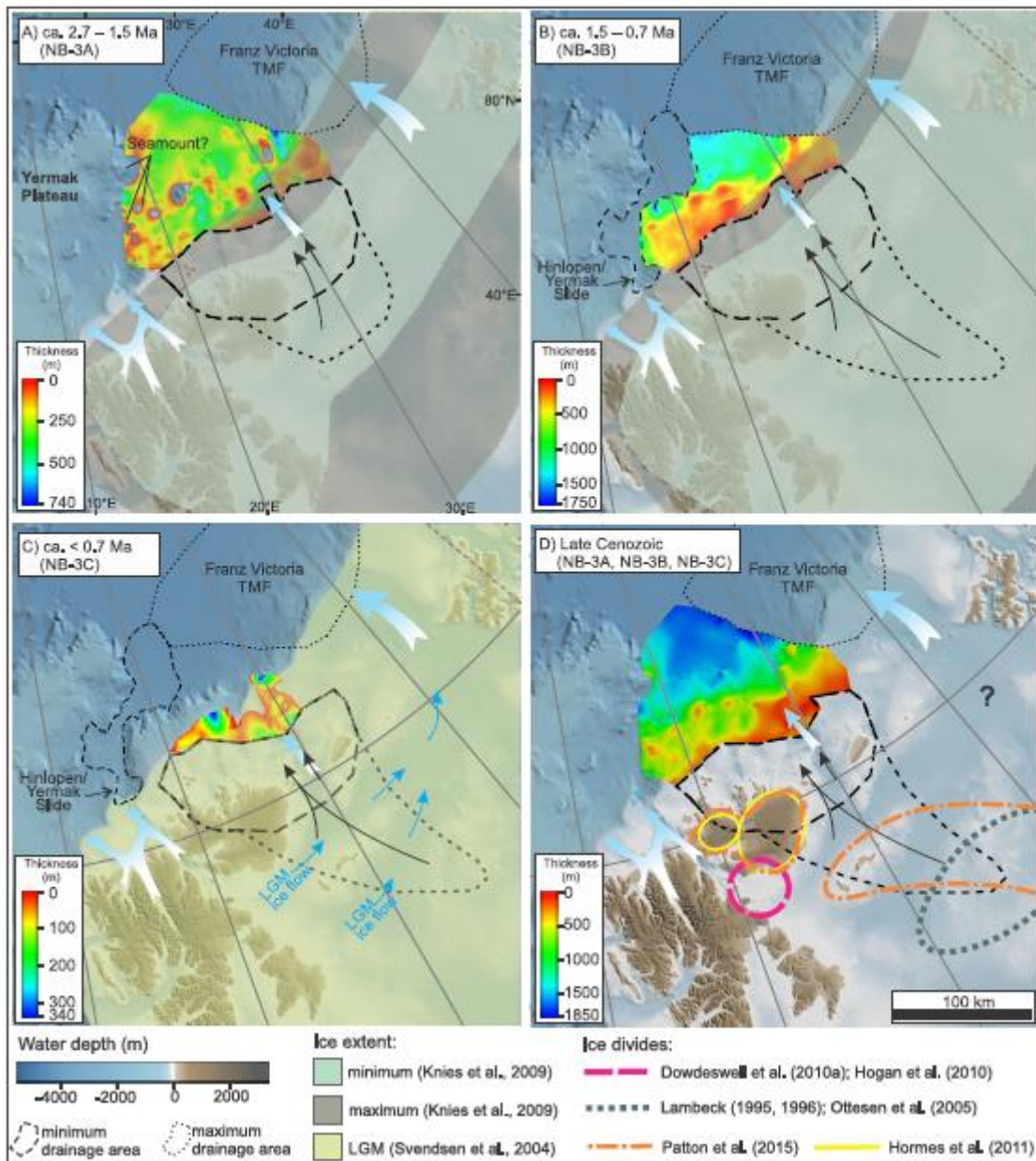


Figure 12. Isopach maps for the glacial sub-units and their inferred drainage areas (minimum and maximum alternative). Bathymetry map is from International Bathymetry Chart of the Arctic Ocean (IBCAO) dataset v. 3.0 Jakobsson et al. (2012) with WGS84 Polar Stereographic Projection. The extent of NB-3A, NB-3B, and NB-3C are delimited by the major Franz Victoria TMF to the east. The alternative drainage areas in this study are following the proposed ice divides in the literature as shown in Figure 12D. Minimum drainage area is following ice dome suggested by Dowdeswell et al. (2010a), Hogan et al. (2010), Hormes et al. (2011), and Patton et al. (2015). Drainage area maximum is based on ice dome inferred by Lambeck (1995, 1996), Ottesen et al. (2005), and Patton et al. (2015). A) NB-3A deposition during ~2.7 – ~1.5 Ma is dominated by ice sheet advanced in the troughs area, particularly in the major troughs (e.g Kvitøya Trough). B) Ice sheet advance continued at the period from ~1.5 to ~0.7 Ma delivering sediment of NB-3B. Kvitøya TMF shows a development of steeply dipping debris. C) From the last ~0.7 Ma, the Kvitøya Trough is inferred to be occupied by fast-flowing ice streams. The distribution of NB-3C is limited only in the axial part of the trough areas. To the west, Hinlopen/Yermak Slide restricted the deposition of this unit. D) The total isopach map from all of the sub-units (NB-3A, NB-3B, and NB-3C).

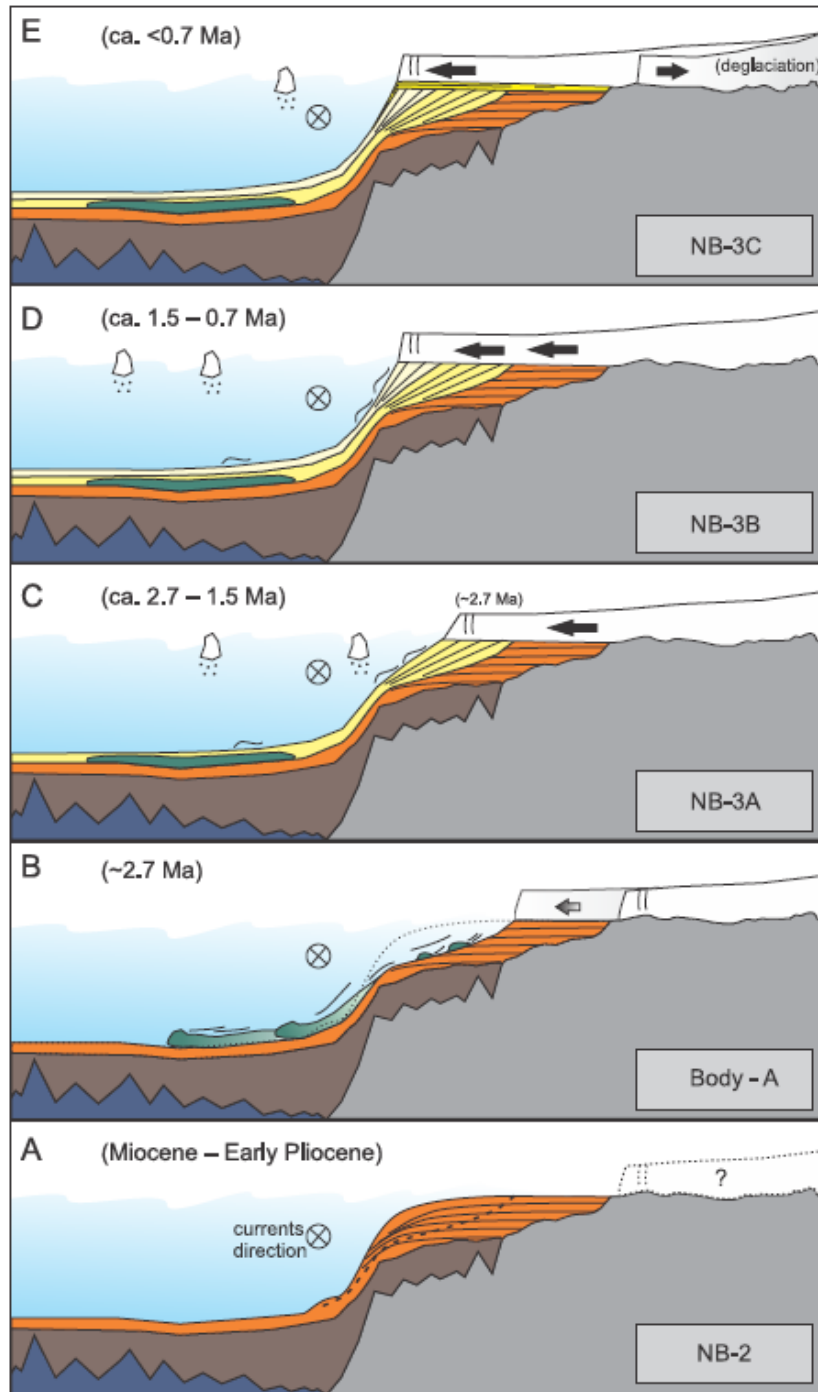


Figure 13. Schematic drawings of Kvitøya TMF development during key phases in the late Cenozoic. A) The deposition of NB-2, which is interpreted as less glacially-influenced contourites and debris materials. Land-based ice might be present (Knies & Gaina, 2008). B) The deposition of Body A. This slope failure may have been occurred just before the deposition of NB-3A. C) The deposition of NB-3A marks the ice sheet advance reaching the shelf break. D) The deposition of NB-3B still represents the progressive seaward movement of ice stream. E) The deposition of NB-3C marks the last stage of ice advance before it retreated during the deglaciation phase.

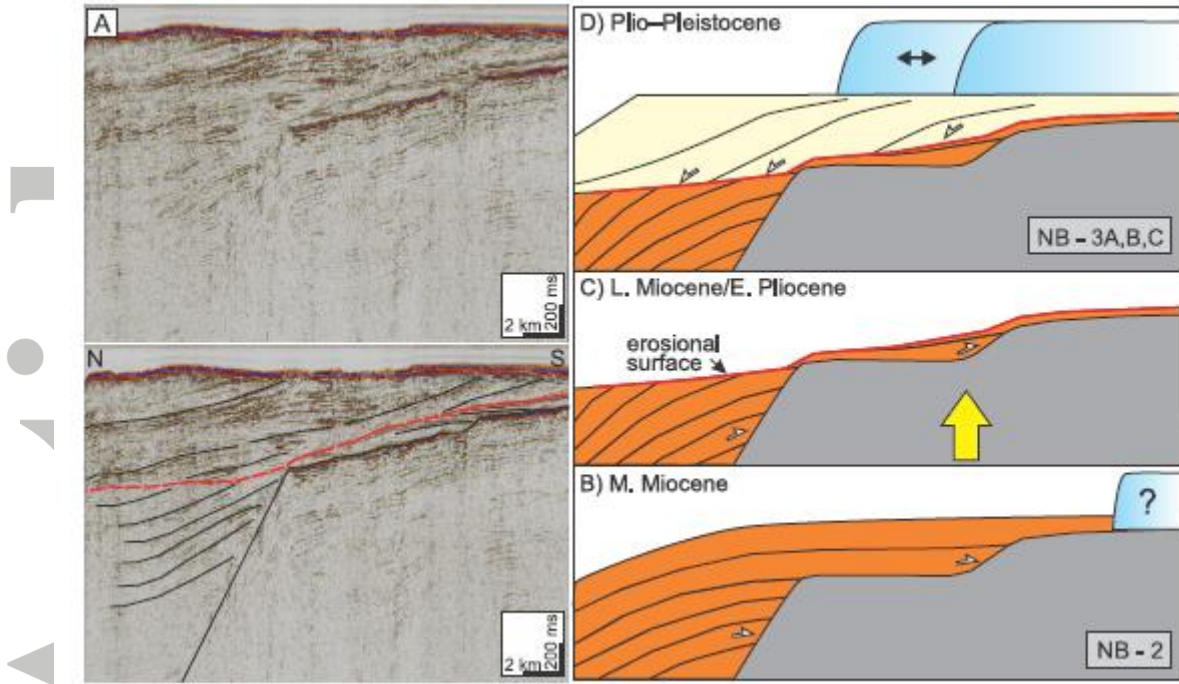


Figure 14. A) Zoom-in profile from Figure 8 at Albertini Trough shows the tectonostratigraphy development around the bathymetric high. B–D) Conceptual figures based on seismic profile (A) illustrating the pre-glacial uplift and erosion in the northeastern Svalbard.

Accepted

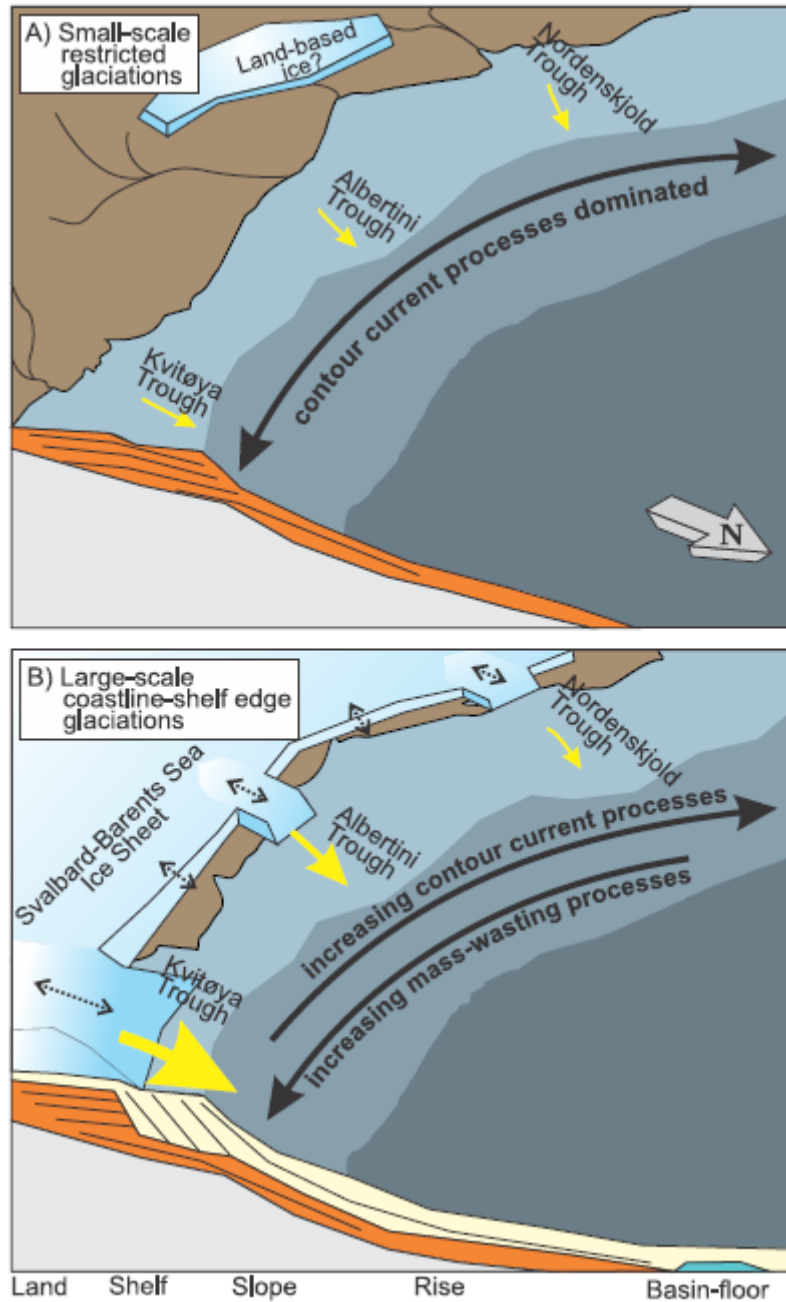


Figure 15. Conceptual model for the northeastern Svalbard – northern Barents Sea continental margin during restricted glaciations and expansive glaciations (sensu Nielsen et al., 2005). The 3D view is referred to Figure 2B. A) Period of small-scale restricted glaciations. A land-based ice over the Nordaustlandet, North East Svalbard is inferred from (Solheim et al., 1998; Knies et al., 2009, 2014). B) Period of large-scale coast-shelf edge glaciations. Ice stream is interpreted to be present in the Kvitøya Trough. Less active ice streams likely occupied the Albertini and Nordenskjold troughs. In the inter-ice stream areas, the dominating processes are the contour currents rather than mass-wasting processes.

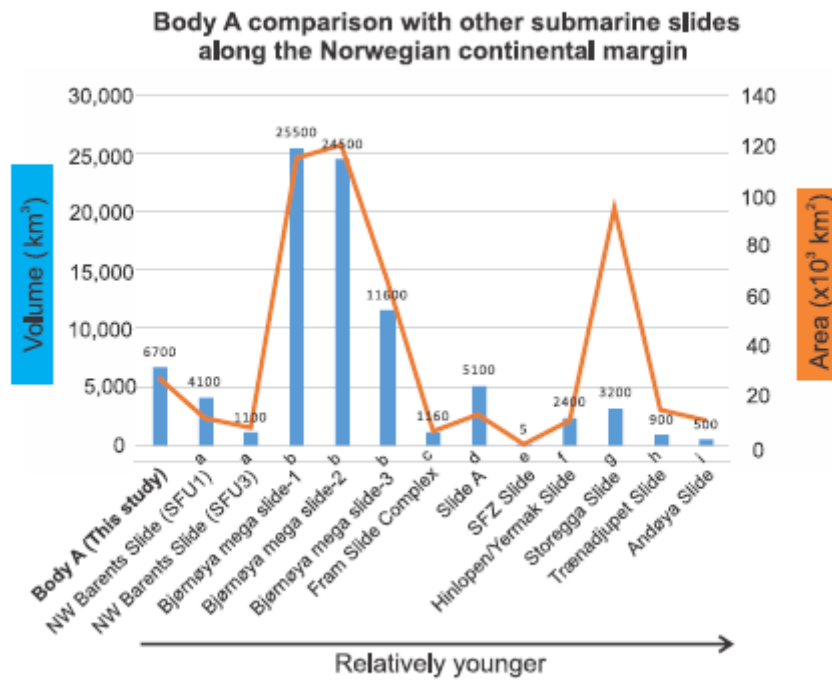


Figure 16. Volume and area comparison for Body A with other submarine slides along the Norwegian continental margin.

Note. ^aSafronova et al. (2015). ^bHjelstuen et al. (2007). ^cElger et al. (2017). ^dLaberg & Vorren, (1996). ^eOsti et al. (2017). ^fVanneste et al. (2006) and Winkelmann et al. (2008). ^gHaflidason et al. (2004). ^hLaberg et al. (2002). ⁱLaberg et al. (2000).